Cranfield Water

Bench-Scale Water Treatment Efficacy Study of PFAS Removal

This report has been prepared for the Department for Environment, Food and Rural Affairs: Drinking Water Inspectorate in accordance with the terms and conditions of appointment for Contract IIT_4373. It was jointly funded by UKWIR Ltd who were part of the Steering Group, along with DWQR Scotland.

Any Enquires relating to this report should be referred to the Client Manager at the following address:

Cranfield University, College Way, Bedfordshire, MK43 0AL

Authors: Peter Jarvis, Irene Carra, Hacer Sakar, Bruce Jefferson, Pablo Campo Moreno, Francis Hassard.

Table of Contents

Nomenclature

5:3 FTCA	5:3 Fluorotelomer carboxylic acid
6:2 FTAB	6:2 fluorotelomer sulfonamide alkylbetaine
6:2 FTSA	6:2 fluorotelomer sulfonate
AOP	Advanced oxidation process
ARP	Advanced reduction process
BV	Bed volume
F-53B	9- chlorohexadecafluoro-3-oxanonane-1- sulfonate
FHxSA	Perfluorohexanesulfonamide
GAC	Granular activated carbon
GenX	Hexafluoropropylene oxide dimer acid
LC-MS	Liquid chromatography mass spectrometry
LOQ	Limit of detection
PFAS	Per and poly fluoroalkyl substances
PFBA	Perfluorobutanoic acid
PFBS	Perfluorobutanesulfonic acid
PFCAs	Perfluoroalkyl carboxylic acids
PFDA	Perfluorodecanoic acid
PFDS	Perfluorodecanesulfonic acid)
PFeCHS	Perfluoroethylcyclohexane sulfonate
PFHxA	Perfluorohexanoic acid
PFHxS	Perfluorohexanesulfonic acid
PFOA	Perfluorooctanoic acid
PFOS	Perfluorooctanesulfonic acid
PFSAs	Perfluoroalkyl sulphonic acids
RSSCTs	Rapid small scale column tests
SMC	Surface modified clay
SPE	Solid phase extraction
WTWs	Water Treatment Works

1. Executive Summary

A range of treatment processes for removal of per and poly fluoroalkyl substances (PFAS) were tested at bench scale. This included:

- Granular activated carbon (GAC) adsorbent
- A surface modified clay (SMC) adsorbent
- Ion exchange (IEX)
- Nanofiltration and reverse osmosis membrane filtration
- Advanced oxidation/reduction processes (AOP and ARP)
- Coagulation

PFAS removal was assessed for a range of different water types: upland and lowland surface water, and groundwater.

PFAS compounds investigated covered a range of chemical structures that differed with respect to their physico-chemical properties (such as their molecular weight, hydrophobicity, chemical functionality and charge).

The aim of the work was to establish the range of PFAS that could be removed by different treatment processes for different source water types. The results were then analysed to recommend which processes should be tested at pilot scale.

GAC: Larger PFAS compounds were preferentially removed over longer periods of treatment. Small PFAS (with 4 carbon atoms) were very poorly removed, being observed in treated water almost immediately. Hydrophobic interactions between the PFAS and the GAC were considered to be the most important removal mechanism, with more hydrophobic PFAS being removed more efficiently.

SMC: Good continuous removal of perfluorooctanoic acid (PFOA) and perfluorooctanesulfonic acid (PFOS) was observed in column tests, although these tests were carried out over a shorter equivalent period than for the GAC. Further tests are required in order to fully understand the extent and range of PFAS removal.

IEX: In initial screening tests, one resin offered the highest potential for removal of PFOA and PFOS. This was taken forward for further testing in continuous scale column tests. Higher equivalent volumes of water could be treated effectively for PFAS removal by IEX than when compared to GAC. Many PFAS types could be treated over long periods without being observed in the treated water. However, as was seen for GAC, the short chain PFAS (with 4 carbons) were seen to break through from the IEX column early into the experimental runs.

While the water matrix had an influence on PFAS removal for GAC, SMC and IEX, no clear trend was observed. Improved removal did not correspond to the water sources with the lowest dissolved organic carbon (DOC) content, suggesting that the type and nature of the DOC plays an important role in competition with PFAS for sorption sites.

Membranes: A range of nanofiltration and reverse osmosis (RO) membranes were tested for PFAS removal using cross flow and dead-end flat configurations. The best performing membranes were able to achieve rejection efficiencies of 99% for many of the PFAS compounds. The most challenging compounds to remove were the short chain PFAS, however the best performing nano and RO membranes were able to remove these by >80%. Given the similar performance between the best nano and RO membrane, the nanofiltration membrane was taken forward for further testing due to the lower operational pressure required for these membranes.

Similarly to that seen for the adsorption processes, background water quality matrix played a role in controlling the removal of PFAS, but this was not in a clear way. There was some indication that the water types with higher DOC levels resulted in reduced removal of some types of PFAS as a result of increased fouling and enhanced concentration polarisation.

AOP and ARP: Most AOPs and ARPs tested did not provide high removal efficiencies (max 30%) at the low UV doses tested. Only photocatalysis showed higher levels of removal for FTAB and FTCA (up to 70%).

Coagulation: Aluminium (Al) based coagulants resulted in the highest removal (>15% for PFOA and >30% for PFOS), with removal being favoured under acidic conditions and high dose. While coagulation is not recommended as a primary process for PFAS removal, the potential for the process to remove a range of compounds is important to acknowledge. Significant concentrations of PFAS may result in water treatment works sludge when PFAS is present in source waters, particularly when Al coagulation is used as a treatment process.

The outcomes from the bench scale testing support the view that the pilot-scale phase of testing should include GAC adsorption, SMC, IEX and nanofiltration membrane separation.

2. Introduction

Per- and polyfluoroalkyl substances (PFAS) are organofluorine compounds with strong chemical and thermal stability. PFAS can exhibit both hydrophilic and hydrophobic properties, making them versatile for diverse commercial applications such as in firefighting foams, non-stick cookware, food packaging materials, water-repellent clothing, stain-resistant fabrics and cosmetics. PFAS can enter surface and groundwater through multiple pathways, including from fire-fighting foam application near airfields, discharge of treated PFAS-contaminated wastewater, runoff from soils, and leaching from landfills. The extensive use and durability of PFAS-containing materials has therefore made PFAS compounds ubiquitous in nature, resulting in their accumulation in the environment and water bodies.

Despite having either been banned or restricted, perfluorooctane sulphonic acid (PFOS) and perfluorooctanoic acid (PFOA) are two of the most prevalent PFAS compounds due to their extensive historical use. Additionally, the development and utilisation of alternative PFAS, as well as precursor compounds and breakdown products, has resulted in the identification of a broad range of compounds in water sources. A range of PFAS have been detected in raw source waters in England and Wales, covering compounds of different molecular weight and structure (Table 1).

Table 1. Most prevalent PFAS compounds detected in raw waters in England and their maximum concentrations (DWI, 2022).

PFAS name	Concentration, µg/L
PFOS	1.86
PFPeA	0.253
THPFOS	0.218
PFOA	0.149
PFHxS	0.09
PFBA	0.072
PFHxA	0.0596
FHxSA	0.0289
PFODA	0.027
PFBS	0.023
PFHpA	0.0123
PFPeS	0.011
FOSA	0.0107
FBSA	0.0105

As a result of the prevalence of PFAS in water sources used for drinking water production, an understanding of how these compounds can be treated is required. The outcomes of the literature review under *Project Deliverable 1* highlighted the potential for PFAS removal using the following treatment processes:

- Membranes: Nanofiltration (NF90, NF270 and DK) and Reverse Osmosis (BW30 and XLE)
- Adsorption: Granular Activated Carbon (GAC) with conventional media (Filtrasorb 400) and a novel surface-modified clay (SMC) media
- Ion exchange: resins A520E, PFA694E, TP109 MP and TP108DW
- Advanced oxidation and reduction processes: UV/sulphite, UV/TiO_2, UV/H_2O_2
- Coagulation

Thus, these processes were selected for bench-scale testing with the aim of understanding their efficiency in removing PFAS from UK water sources. While significant research is being developed globally on PFAS removal, limited focus has been placed on UK water sources, despite the strong influence of water quality on removal efficacy. Therefore, the selected bench scale processes were tested using UK groundwater, upland water and lowland water sources to assess the influence of background water composition on PFAS removal.

2.1. Aim and Objectives

The aim of this research was to investigate the most suitable processes for the removal of PFAS compounds from UK drinking water sources. The results will then be used to inform on the design of the subsequent pilot testing phase.

3. PFAS model compounds

The PFAS compounds were selected considering their prevalence in UK source water and to represent a broad range of physicochemical properties which influence their treatability, including chemical functionality, chain length, hydrophobicity and charge (Table 2). These properties are expected to influence removal mechanisms such as size exclusion, diffusion, electrostatic interactions and hydrophobic interactions. During the bench-scale testing the model compounds were spiked at an equimolar concentration of 0.4 nM for each PFAS (equivalent mass concentration provided in Table 2), unless otherwise stated.

Table 2. Selected PFAS model compounds and physicochemical properties.

Group	Subgroup	Functional group	compound	Molecular weight g/mol	Mass concentration for 0.4 nM (ng/l)	number of C	Charge	pKa	logKoc	Structure
Perfluoroalkyl acids	Perfluoroalkyl carboxylic acids (PFCAs)	$-COO^-$	Perfluorobutanoic acid (PFBA)	214.04	85.6	4	negative	1.07	1.9	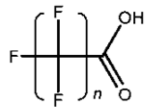
			Perfluorohexanoic acid (PFHxA)	314.05	125.6	6	negative	-0.78	1.3	
			Perfluorooctanoic acid (PFOA)	414.07	165.6	8	negative	-4.2	1.89-2.63	
			Perfluorodecanoic acid (PFDA)	514.08	205.6	10	negative	-5.2	2.76-2.96	
	Perfluoroalkyl sulphonic acids (PFSAs)	$-SO3^-$	Perfluorobutanesulphonic acid (PFBS)	300.1	120.0	4	negative	-3.31	1.2-1.79	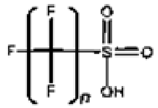
			Perfluorohexanesulphonic acid (PFHxS)	400.11	160.0	6	negative	-3.32	2.4-3.1	
			Perfluorooctanesulphonic acid (PFOS)	500.13	200.1	8	negative	-3.32	2.4-3.7	
			Perfluorodecanesulphonic acid (PFDS)	600.13	240.1	10	negative	-3.24	3.53-3.66	
Perfluoroalkyl ether acids	Perfluoroalkyl ether sulphonic acids	-SOO-	9- chlorohexadecafluoro-3-oxanonane-1- sulphonate (F53B)	532.6	213.0	8	negative	-3.25	4.1	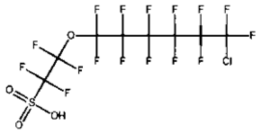
	Perfluoroalkyl ether carboxylic acids	-COO−	Hexafluoropropylene oxide dimer acid (GenX)	330.19	132.1	6	negative	-0.77	1.7	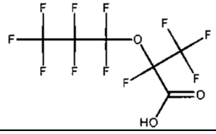
Fluorotelomer substances	Fluorotelomer carboxylic acids	COOH	5:3 Fluorotelomer carboxylic acid (5:3 FTCA)	342.1	136.8	8	negative	NA	NA	
	Fluorotelomer sulphonic acids	$-CH_2CH_2SO_3-$	6:2 fluorotelomer sulphonate (6:2 FTSA)	428.16	171.3	8	negative	-2.72	2.1	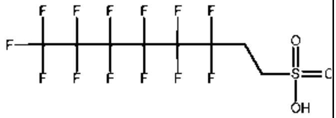
	Fluorotelomer sulphonates	SO3	Perfluoroethylcyclohexane sulphonate (PFeCHS)	461.13	184.5	8	negative	-3.11	2.5	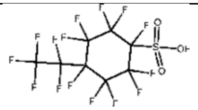
	Fluorotelomer sulphonamide alkyl betaine	(-CO2-)	6:2 fluorotelomer sulphonamide alkylbetaine (6:2 FTAB)	570	228.0	6	Zwitterionic	2.81	2.4	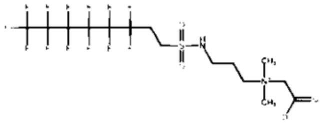
Perfluoro alkane sulphonamides	Perflorohexane sulphonamide	$-SO_2NH_3$	Perfluorohexanesulphonamide (FHxSA)	399.13	159.7	6	neutral	3.37	2.3	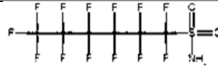

4. Water characterisation

Six water matrices were investigated in this study, three groundwaters, one upland water and two lowland waters (Table 3). All waters were spiked with 0.4 nM of PFAS except Groundwater 3 which was already contaminated with a high concentration of several PFAS. Due to the constraints associated with the available number of samples for full PFAS analysis, some tests were performed using only PFOS and PFOA as two of the most abundant PFAS in water sources (Table 2), while other experiments analysed a combination of the 15 PFAS model compounds. This approach enabled an understanding of whether a process had the potential for PFAS removal. Further testing enabled exploration of removal for a wider range of PFAS.

Table 3. Characterisation of the water sources tested.

Source water	**pH**	**UV_{254} (cm^{-1})**	**DOC (mg/L)**	**Turbidity (NTU)**	**Conductivity (µS/cm)**
Groundwater 1	8.17	0.043	1.3	0.35	480
Groundwater 2	7.86	0.02	1.3	0.04	236
Groundwater 3	7.2	0.044	1.1	0.22	151
Lowland water 1	8.36	0.061	3.7	0.08	463
Lowland water 2	8.3	0.13	4.2	0.24	586
Upland water	6.1	0.184	3.5	0.42	32

4. PFAS analysis and chemicals

PFAS standards were supplied by Greyhound Chromatography (Wallasey, England). Water samples for PFAS analysis were sent to RPS Laboratories (Bedford, England) for external analysis. The full set of model compounds were analysed by RPS using a UKAS accredited method for 51 fluorinated and perfluorinated compounds, with limits of detection (LOQs) down to 0.1 ng/L for most compounds, and a summed reporting limit for all 51 compounds of 25 ng/L. The method uses 250 mL of sample, which is acidified, purified and concentrated. Samples were further concentrated using specialised solid phase extraction (SPE) cartridges. Extracts were analysed by liquid chromatography mass spectrometry (LC-MS/MS) in negative electrospray ionisation mode. A smaller subset of samples were analysed in-house at Cranfield University following a modified version of USEPA method

8327 for the analysis of PFOA and PFOS in drinking water by direct sample injection into LC-MS/MS.

5. Adsorption

GAC is a conventional treatment process widely used in the production of potable water. Thus, several studies have investigated the efficiency of this process for the removal of PFAS. In this work, rapid small scale column tests (RSSCTs) were performed to understand the efficiency of conventional GAC for PFAS removal. This approach provides a much closer representation of how the media might perform during continuous operation, while utilising much less media and water, but does require the media to be crushed to a smaller particle size. For the clay-based media (SMC), this was used as supplied because crushing the granules may have damaged its structure and hence reduced the adsorption capacity (although subsequent discussion with the manufacturer suggested that crushing the SMC would be suitable for further testing in RSSCTs). As a result, the SMC treated a much lower number of equivalent bed volumes than when compared to the GAC. Kinetic batch tests were subsequently performed to evaluate the influence of the water matrix on the efficiency of adsorption.

5.1 Methodology

RSSCTs followed the methodology described in Standard Practice for the Prediction of Contaminant Adsorption on GAC in Aqueous Systems Using RSSCTs (American Society for Testing and Materials Standard Method D-6586-03). The design of the RSSCTs was based on a constant diffusivity model (Crittenden et al., 1991). A conventional bituminous coal-based activated carbon manufactured by Chemviron Carbon Ltd - Filtrasorb 400 (F400) and a modified bentonite clay media SMC were tested. GAC F400 is widely used in the water sector as an adsorbent and SMC is a novel new media that has shown efficient PFAS removal in case studies in the US (Murray et al., 2023).

The media was manually ground with a pestle and mortar and sieved using standard sieves with mesh sizes of 80 and 100 to obtain the desired particle diameters for small columns. Ground samples were sonicated to remove fine particles and prevent blockages and the build up of head pressure during testing. The GAC samples were rinsed until a clear water stream was observed. Once rinsing was finished, the media was dried in the oven at 35 °C.

The media was placed in a 10 mm inner diameter column with polypropylene caps and fittings (Diba Omnifit Chromatography Columns, Cole-Parmer Ltd, UK) (Figure 1). The column diameter (10 mm) and bed height were designed to minimise channelling effects such that the ratio of the column diameter to the media particle diameter was greater than 50

(Park et al., 2020). For the SMC tests, as previously noted, the media was used as supplied. This test did not, therefore, meet the criteria as stated above, but allowed an initial assessment of the media to be made using the same apparatus, alongside treatment of a significant number of bed volumes of water to establish its suitability for further tests.

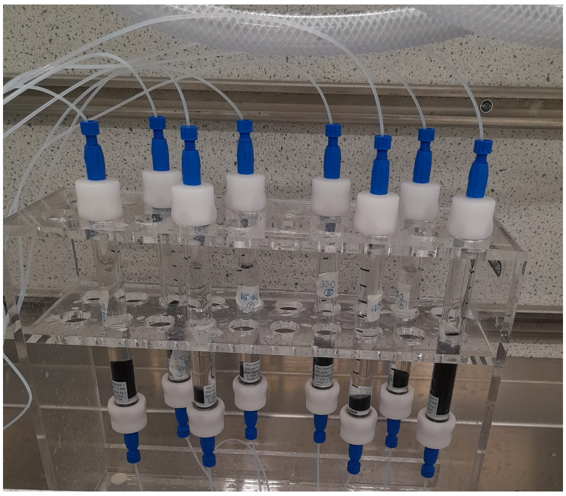

Figure 1. RSSCT experimental setup.

Columns were run in duplicate for each tested condition and 8 columns were run in parallel. Water was pumped from a storage tank using a peristaltic pump (Watson Marlow 323 Series) at a rate of 5 mL/min. GAC F400 was tested at 20 min EBCT to mimic typical operating conditions in the UK. SMC was tested at 5 min EBCT as suggested by the manufacturer. The calculation of the number of bed volumes was estimated based on the set flow rate without considering small flow fluctuations during testing.

Kinetic tests were performed in batch experiments in 1 L flasks with a media concentration of 50 mg/L. Then the flasks were agitated for 1 hour with an orbital shaker (Stuart Orbital Shaker, Bibby Scientific Ltd., Staffordshire, UK) at a rate of 250 rpm.

5.2 Adsorption

At 20 min EBCT, PFAS with a carboxylic acid functional group started to show breakthrough at around 10,000 BV for the compounds with 6 or more carbon atoms in the chain (C6-C10), with longer chain compounds being better removed than the shorter PFAS (Figure 2a). The smaller PFBA (C4 compound) was removed the least efficiently and broke through the column immediately. For PFAS with a sulphonic acid group, breakthrough took place after 13,000 BVs for compounds with chain lengths C4-C8. The exception was for PFDS (a long chain compound, C10) which broke through early in the trial. This was unexpected as most studies have shown increased removal with increasing length of the PFAS molecule as the hydrophobicity of the compound increases. Previous literature supports the view that GAC has higher capacity for longer chain PFAS (Park et al., 2020). This is because longer PFAS chain lengths have a greater hydrophobicity for a given functional group, and hence typically have a greater number of BVs before breakthrough. To support this, a logarithmic relationship has been found between the octanol partition coefficient of carboxylic PFAS and the BVs required to achieve 50% concentration to breakthrough (Park et al., 2020,) implying that hydrophobic interactions play a key role in the removal of PFAS through adsorption by activated carbon. The results observed for PFDA were therefore not expected and are discussed further following the kinetics section.

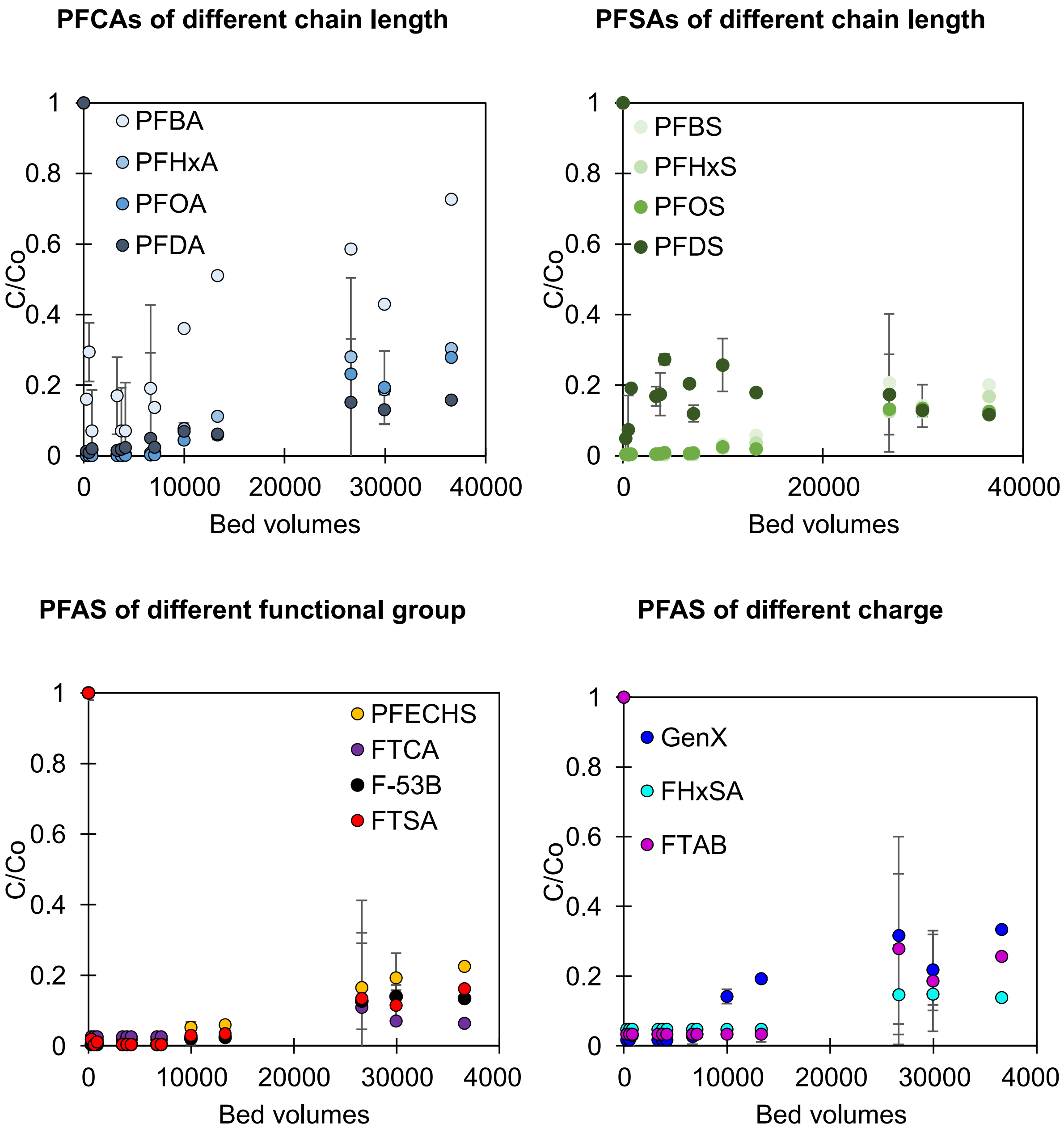

Figure 2. PFAS concentrations during RSSCTs with GAC F400 at 20 min EBCT for groundwater 1. The PFAS compounds were spiked at a concentration of 0.4 nM. The results are grouped by PFCAs (a); PFSAs (b); PFAS of different functional group (c); and PFAS with negative (GenX), zwitterionic (FTAB) and neutral (FHxSA) charge (d).

PFAS of different chemical functionality including an alkyl ether sulphonic acid, and fluorotelomers with carboxylic, sulphonic and sulphonate groups followed similar trends to the sulphonic acid group, reaching around 13,000 BVs before significant breakthrough took place (Figure 2c). When looking at compounds of the same chain length but with different charge [GenX (negative), FTAB (zwitterionic) and FHxSA (neutral)], GAC F400 had the lowest capacity for the negatively charged GenX compound, with breakthrough occurring at

10,000 BVs (Figure 2d). The neutral FHxSA and zwitterionic 6:2 FTAB had a similar breakthrough profile, occurring after approximately 20,000 BVs. For all three types of PFAS, removal levels remained between 70-90% for the duration of the trial. This further supports the view that removal mechanisms are more dominated by hydrophobic interactions rather than electrostatic interactions. An initial column test using SMC at 5 min EBCT (Figure 3) showed good continuous removal of both PFOS and PFOA and that further removal would be expected beyond 9,000 BVs. Due to the difference in particle size between SMC and GAC (SMC was not crushed), a lower number of equivalent BVs were treated during the former test, but this was extended in the subsequent pilot trials.

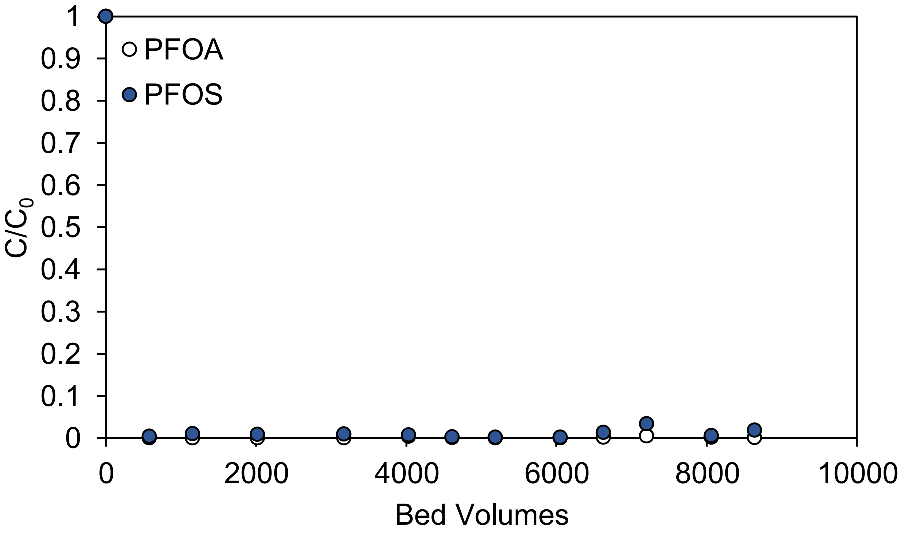

Figure 3. PFOS and PFOA concentrations during RSSCTs using SMC at 5 min EBCT. Both PFAS were spiked at 0.4 nM into groundwater 1.

Tests were performed over one hour of adsorption with both GAC and SMC (Figures 4 and 5) to compare the effect of different water matrices on PFAS uptake (see Table 3 for water quality characteristics). It is acknowledged in these tests that adsorption equilibrium was unlikely to have been reached for any of the media, but served as a useful way of showing how water matrix influenced the removal of different PFAS compounds. These data should therefore not be used to predict how much PFAS might be adsorbed for any given condition in real world systems. For both GAC and SMC, carboxylic acid PFAS removal efficiency increased as the carbon chain length increased (PFBA<PFHxA<PFOA<PFDA). A similar trend was observed for sulphonic PFAS except for PFDS (10C), which for some of the water sources was less well removed than PFOS (8C) when using GAC (PPFBS<PFHxS<PFDS<PFOS) (Figure 4b). For SMC, the removal of PFDS was similar or slightly higher than for PFOS. The reduced removal when using GAC aligns with the results

from the RSSCT column tests that saw lower removal of the longer chain PFAS compound. One hypothesis for this may have been that the larger PFAS was size excluded from accessing the GAC pores. However, this was not consistent with the literature, or the results observed for PFDA, equivalent in chain length to PFDS but with a carboxylic acid group. Competing organic compounds in the background matrix may have been responsible for the reduced removal, but this requires further work to elucidate the mechanisms causing the difference.

Overall, the sulphonic PFAS compounds of equivalent chain length were more effectively removed than the carboxylated forms. Removal of carboxylic acid PFAS were similar or slightly higher for the higher MW compounds when using SMC in comparison to GAC, with removals ranging from 15-50% for PFOA, 5-30% for PFHxA, and 30-70% PFDA. For the smaller PFBA, removal across the different water types was low but more consistent for GAC in comparison to SMC (removals between 3-20%). For sulphonated PFAS, a greater difference in removal was seen between GAC and SMC, where the latter achieved higher removal. GAC resulted in removal rates between 20-68% for PFOS, 10-20% for PFBS, 10-63% for PFHxS, and 20-65% for PFDS. While SMC led to removal ranges of 50-80% for PFOS; 10-29% for PFBS, 22-73% for PFHxS, 34-82% for PFDS. Murray et al. (2023) have suggested that the higher removal rates of shorter chain acidic PFAS and PFAS with moderate hydrophobicity using SMC may be attributed to electrostatic interactions with cationic functional groups on the adsorbent surface. This contrasts with longer chain PFAS, where hydrophobic interactions seem to be the main driving mechanism.

While the water matrix had an influence on PFAS removal for both GAC and SMC, no clear trend was observed, although removal tended to be higher for groundwater 1, lowland water 1, and lowland water 2. It was not the case that the water type with the highest background DOC resulted in the lowest PFAS removal, indicating that the nature of the organic matter played an important role in competition processes for adsorption sites on the media tested.

When comparing PFAS compounds of different functional group (Figures 4c and 5c), FTCA was similarly removed by GAC and SMC for a given water source. F-53B, which also has 8C in its chain and is an ether sulphonic acid PFAS, was more efficiently removed by SMC, with removal rates between 50-84% versus 15-58% removal when using GAC. Similar removal of between 10-50% was seen for FTSA between GAC and SMC.

GenX (negative), FTAB (zwitterionic) and FHxSA (neutral) showed removals of up to 45% by GAC, while removals of <30% were seen with SMC (Figures 4d and 5d). One exception was the higher removal of FHxSA (>50%) from groundwater 2 for both GAC and SMC. In all cases, the negatively charged GenX was removed the least efficiently in comparison to the other two compounds, suggesting that electrostatic interactions and charge-based mechanisms were less relevant for these compounds, and hydrophobic interactions were more likely to drive separation. This was further supported by the log K_{oc} value, which was lowest for GenX (0.77, Table 2).

Overall, 6-8C PFAS were better removed than lower chain (4C) PFAS for the same functional group (for example, PFOS vs PFBS). Separation mechanisms by adsorption were more strongly driven by hydrophobic interactions, although electrostatic interactions play a role for smaller chain PFAS such as PFBA, and size exclusion could interfere with the removal of larger compounds such as PFDS. It is worth noting that when comparing between conventional GAC and SMC removal efficiencies depended on the PFAS group, relating to the specific mechanisms driven by each media surface. These results indicate that the functional groups and the adsorbent structure play a significant role on removal mechanisms. Hence, interaction between PFAS of different functionality and background organic matter of different composition play an important role in controlling PFAS removal. However, there is limited research that explains the driving separation mechanisms for PFAS other than for the carboxylic acids and the sulphonic acids. This is an area that requires attention in future research.

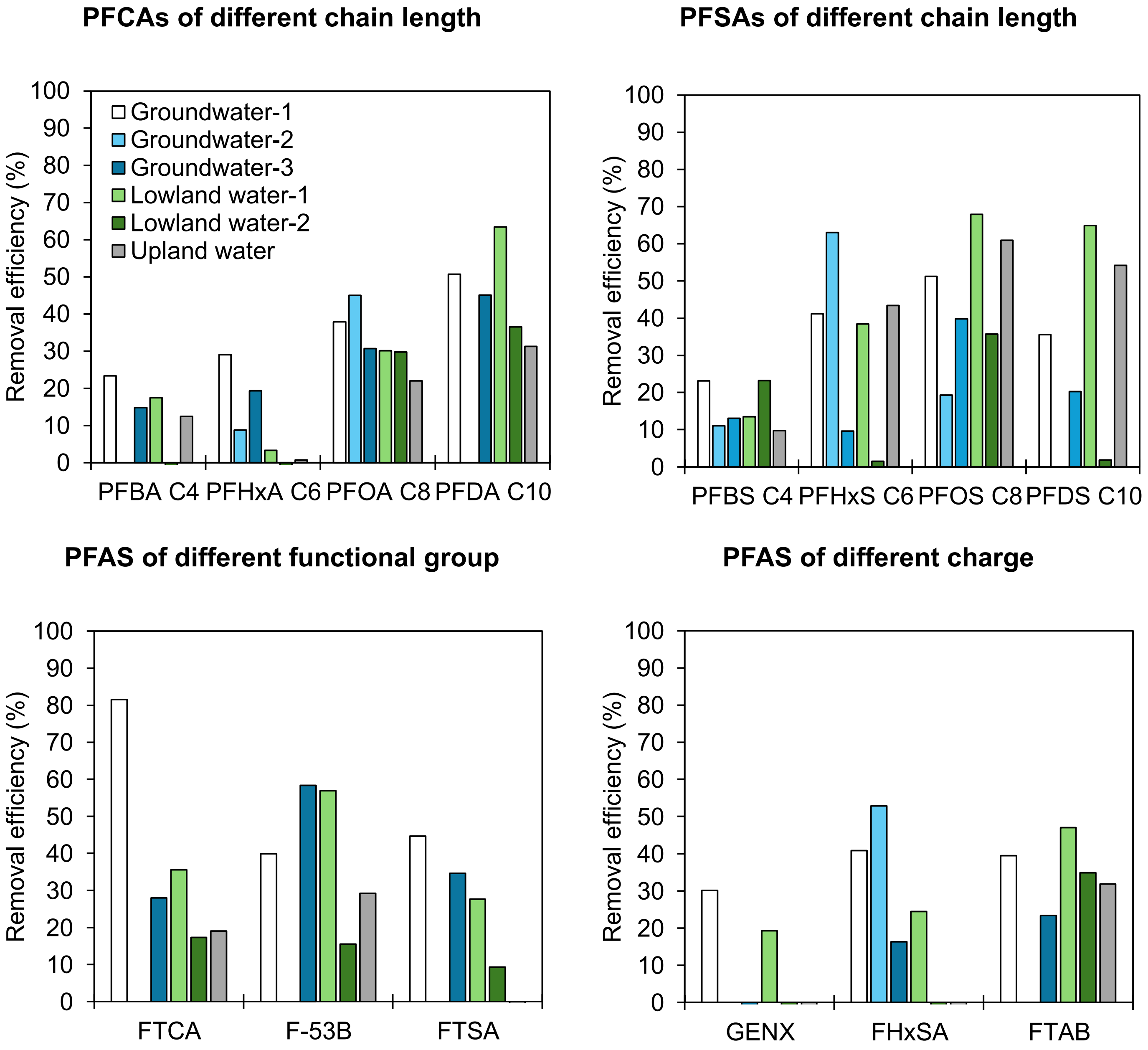

Figure 4. PFAS removal after 60 min adsorption batch tests using GAC in groundwaters 1-3, lowland waters 1-2 and upland water. PFAS were spiked at 0.4 nM.

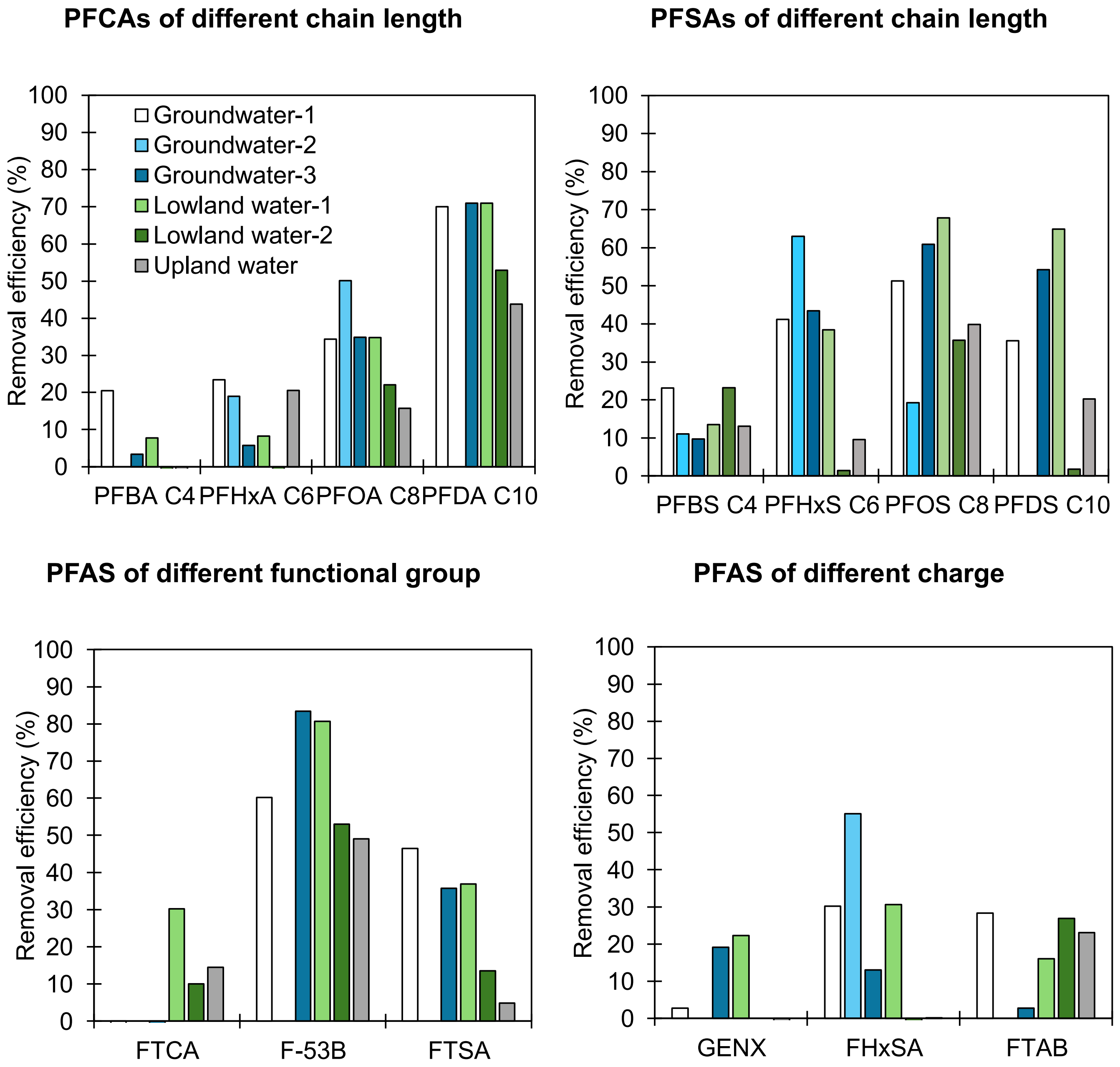

Figure 5. PFAS removal after 60 min adsorption batch tests using SMC in groundwaters 1-3, lowland waters 1-2 and upland water. PFAS were spiked at 0.4 nM.

6. Ion exchange

Ion exchange has been reported as an effective treatment for PFAS removal from drinking water sources. Most of the resins used for this purpose are those that have a polystyrene matrix and are either macroporous or gellular in structure. The literature review highlighted four resins which have been shown to have some of the highest PFAS removal efficiencies. These resins were selected and taken forward for the bench scale testing, with the results reported below.

6.2 Methodology

Ion exchange experiments were performed with Lewatit Monoplus TP109 MP, Lewatit TP108 DW, Purolite A520E and Purolite PFA694E (Table 4).

Table 4. Properties of the selected IEX resins for testing.

Structure	**Resin name**	**Resin type**	**Functional group**	**Resin matrix**
Macroporous	Lewatit® MonoPlus TP109 MP	Strong base anion exchange	Quaternary ammonium	Polystyrene
	Purolite A520E	Strong base anion exchange	Triethyl quaternary amine	
Gel-type	Lewatit® TP108		Quaternary ammonium	
	Purolite PFA-694E	PFAS selective	Complex amino group	

Preliminary kinetic batch experiments were conducted over 60 min in 100 mL polypropylene flasks to compare the performance of the resins in removing PFAS (Figure 6). The flasks were agitated on a shaker (Stuart Orbital Shaker, Bibby Scientific Ltd., Staffordshire, UK) at a rate of 250 rpm. Groundwater 1 was used for the testing using 1 g/l resin and spiked with 0.4 nM PFOS and PFOA. To investigate the effect of the resin concentration on PFAS removal, batch experiments were carried out at 0.1 and 1 g/L for each of the resin types using groundwater 1 as the text matrix spiked with 0.4 nM PFOS and PFOA. The contact time between the resin and the water was 24h. To evaluate the effect of the background water matrix, the four resins were then tested using ground- and surface water.

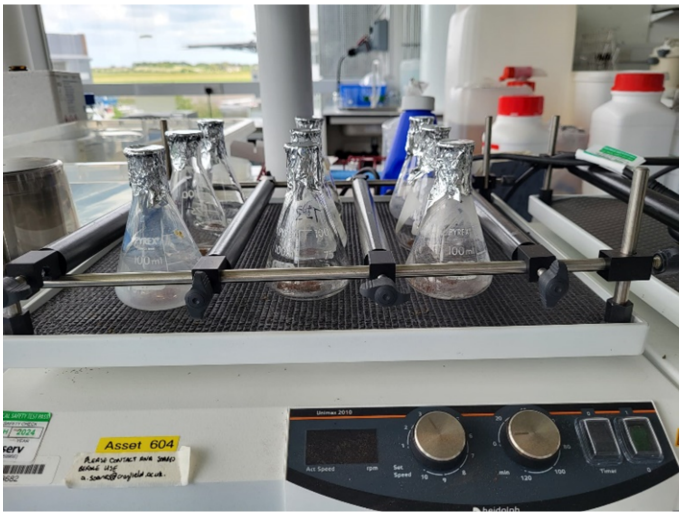

Figure 6. Ion exchange experimental setup.

Following the batch testing, RSSCTs experiments were also performed using the same method as described in Section 5.2. This was following published guidance on the appropriateness of using crushed ion-exchange media in RSSCTs (Schaefer et al., 2020).

6.3 Results

Batch kinetic tests showed gellular resins PFA-694E and TP108 achieved 81-87% removal, while macroporous TP109 and A520E resulted in 93-99% removal after 60 min (Figure 7). The best performing resin was TP109, which is PFAS-selective, and achieved 90 and 99% removal for PFOA and PFOS, respectively. The TP109 resin was also much faster in removing PFOS compared to the other resins, reaching near complete removal after just 20 minutes, while the best removal was not seen until 60 minutes for the other resins. The rate of removal was much more similar for all resins for PFOA.

While the resin structure (microporous versus gellular) influences properties such as porosity and capacity, it has been reported that the hydrophobicity of the exchange functional group in the IEX resin has a strong link with the capacity of the resin in removing PFAS, even more so than resin structure. For example, trimethyl quaternary ammonium groups have been reported to show higher capacity for PFAS removal in comparison to triethyl quaternary amines, which are less hydrophobic (Zaggia et al., 2016).

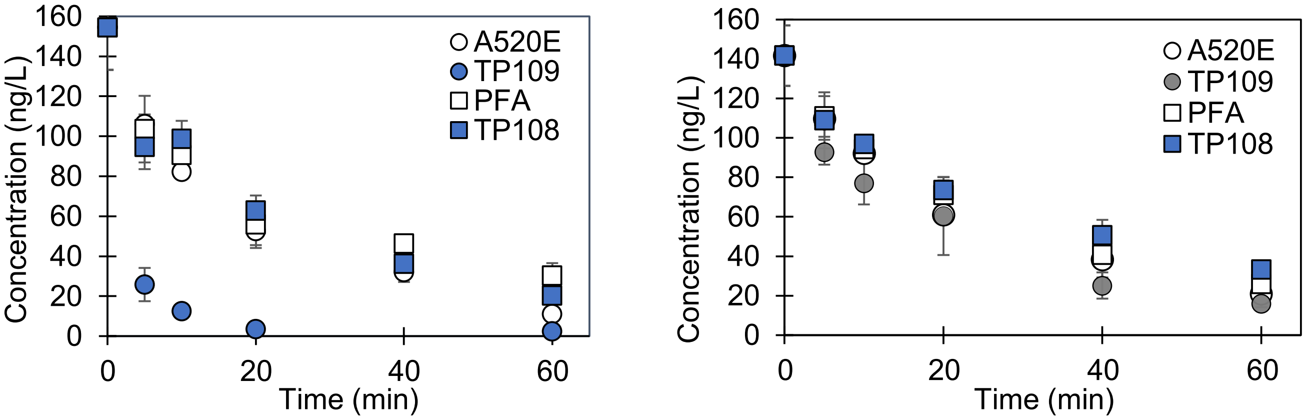

PFOS **PFOA**

Figure 7. Removal of PFOS and PFOA in 60 min kinetic bath tests time for a range of IEX media. Macroporous resins are marked with circles and gellular resins with squares.

The resin with the best separation performance (Lewatit Monoplus TP109 MP) was taken forward for further testing over a longer time to understand when a pseudo equilibrium removal could be achieved (Figure 8). Equilibrium was achieved at 50 min for PFOS and after 90 min for PFOA. Sulphonic PFAS are typically observed to be better removed by IEX than their carboxylic acid equivalent compounds. This is because sulphonic groups are more negatively charged, and they create stronger electrostatic interactions compared to carboxylic groups (Zaggia et al., 2016). An interesting observation was that after 120 min, a small amount of desorption of both PFOS and PFOA was detected, increasing the residual concentration of PFOS from a minimum of <0.5 ng/L to 3.5 ng/L, while for PFOA this increase was from 1 ng/l to 2 ng/L. The new concentrations then reached a new equilibrium. After 24 h, the removal efficiencies were recorded as 99% for PFOA and 95% PFOS. Desorption is a phenomenon that has been previously reported for PFAS chemicals, particularly for shorter chain compounds, as more thermodynamically stable molecules displace already sorbed compounds. While it was not clear which background constituent caused this displacement, the results highlighted the risk of PFAS concentration increases in treated water in sorption processes at long contact times because of desorption.

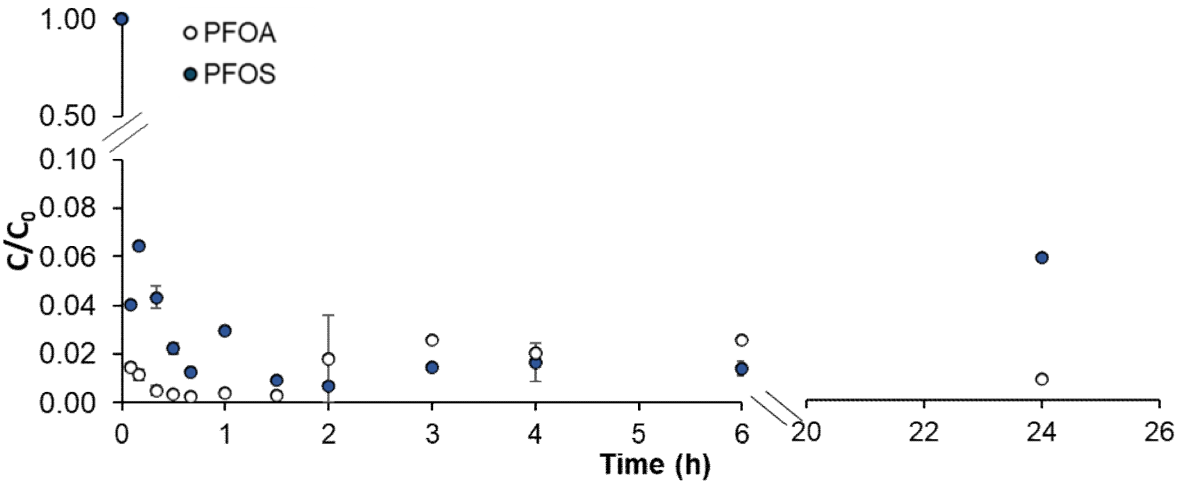

Figure 8. Concentration of PFOS and PFOA in water during batch kinetic testing using TP109 MP IEX resin at a resin dose of 1 g/L in groundwater 3.

In order to investigate the effect of PFAS chain length, different functional group and charge on removal by ion-exchange, the TP109 MP resin was tested using groundwater 2 (Figure 9). For PFCAs and PFSAs, when 1 g/L resin concentration was used, all compounds were removed to below the limit of detection. For 0.1 g/L all compounds were removed by more than 85%. The PFBA (4C), PFDA (10C) and PFOS (8C) had slightly lower removal, but this was nevertheless still high. There was minimal impact of molecular weight on removal efficiency for either sulphonic or carboxylic acid PFAS with differences in removal likely explained by the lower resin dose, and the available surface area for sorption.

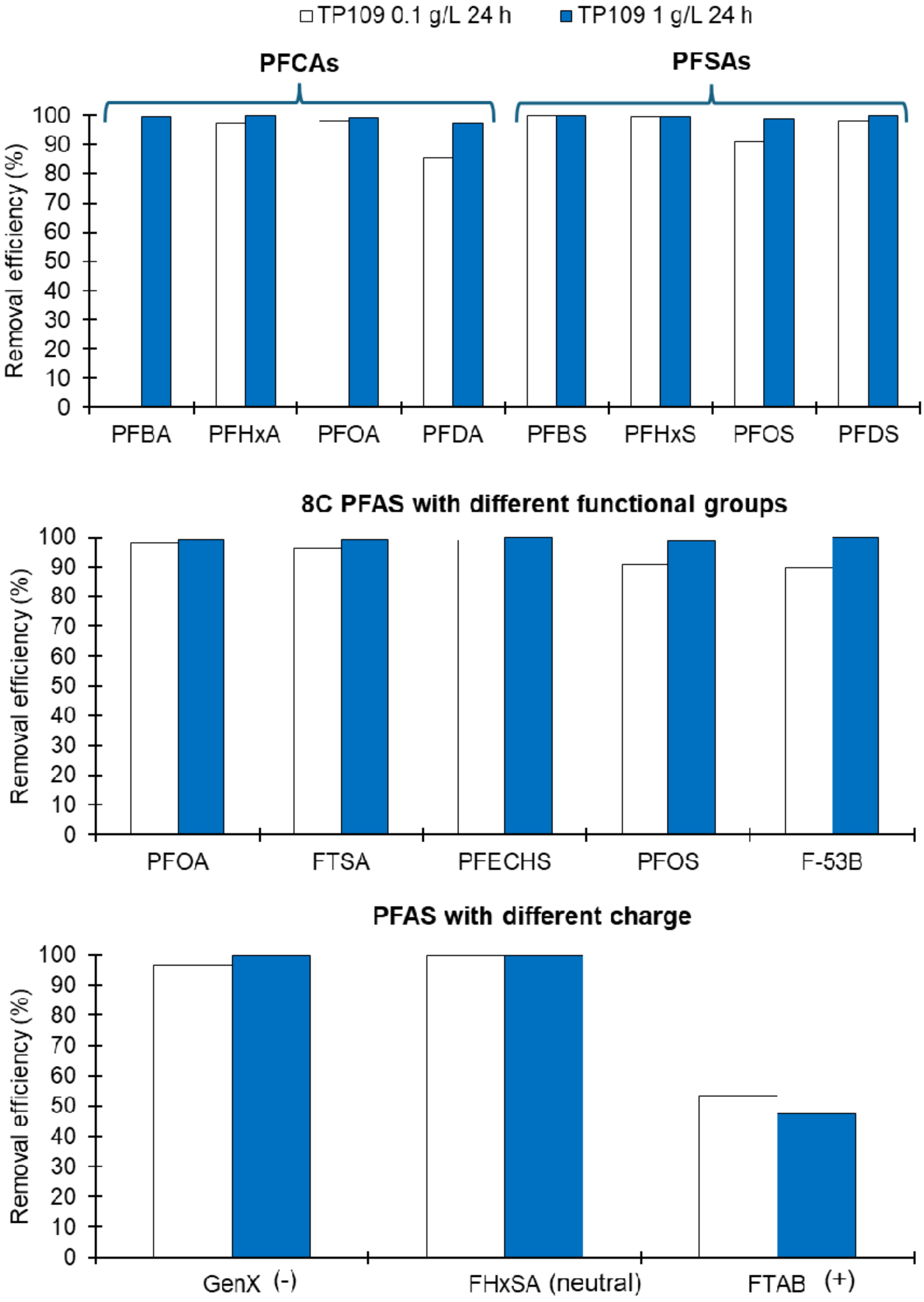

Figure 9. Removal of PFAS by IEX resin TP109 at 0.1 and 1 g/L resin concentrations after 24 hours contact time. PFAS were spiked at 0.4 nM concentration into groundwater 1.

Similar tests were performed with PFAS of different functional group but the same carbon chain length (8C) (Figure 9). At the highest resin concentration, near complete removal of all PFAS was observed. At the lower resin dose, PFOS and F-53B were slightly less well removed at between 89-90%. In the case of PFECHS, its structure has a fully fluorinated six-carbon ring with a 2-carbon tail which might favour its adsorption through an increase in the molecule's hydrophobicity (MPART, 2020).

When comparing the influence of molecular charge on IEX efficiency (Figure 9), both GenX (negatively charged) and FHxSA (neutral) were removed above 97% at both resin concentrations. Electrostatic and hydrophobic interactions are important during removal of PFAS by IEX processes. It should be noted that although FHxSA is a zwitterionic compound with a net charge of zero, it still carries positive and negative charges. As such the latter can drive anionic exchange mechanisms as well as hydrophobic interactions, which would explain the high removal observed. On the other hand, the positively charged FTAB was less well removed at ca 50% owing to increased electrostatic repulsion. In the case of FTAB, the limited removal observed was therefore most likely driven by adsorption/hydrophobic mechanisms.

The efficiency of IEX as a treatment option for the removal of PFAS was further investigated through RSSCTs using the TP109 resin (Figure 10). PFCAs were efficiently removed for 16,000 BVs apart from the short chain PFBA (4C), which showed some breakthrough from the beginning of the tests. Similarly to results seen for GAC adsorption, short-chain PFCAs have been reported to be less efficiently removed by IEX (Zaggia et al., 2016). PFSAs were removed by more than 83,000 BVs except for PFDS, which broke through earlier, consistent with the results obtained during the adsorption RSSCTs. When looking at other functional groups, FTCA showed breakthrough before 10,000 BVs, followed by FTSA. Negatively charged GenX showed breakthrough at 16,000 BVs. Mirroring the kinetic test results, positively charged FTAB was poorly removed by IEX.

It has been postulated that hydrophobic interactions strongly drive PFAS removal by IEX, similarly to that seen during adsorption by GAC, in addition to charge-driven ionic interactions. This supports the higher removal observed for longer chain PFCAs and PFSAs since their hydrophobicity is higher than for shorter chain compounds. The hydrophobic interactions of long chain PFAS can result in the formation of micelles and aggregates on the surface of the IEX resin (Gao et al., 2017). The formation of these micelles and aggregates has been suggested to further improve removal by capturing additional compounds within the micelle layers on the resin. It should be noted, however, that beyond the present case there is a lack of information regarding hydrophobicity of less studied PFAS such as fluorotelomers (FTAB, FTCA) or F-53B. Furthermore, there is little information published regarding these compounds and their potential to be removed from water by any treatment process. The data presented here therefore provides some useful empirical evidence for removal of these different types of PFAS compound.

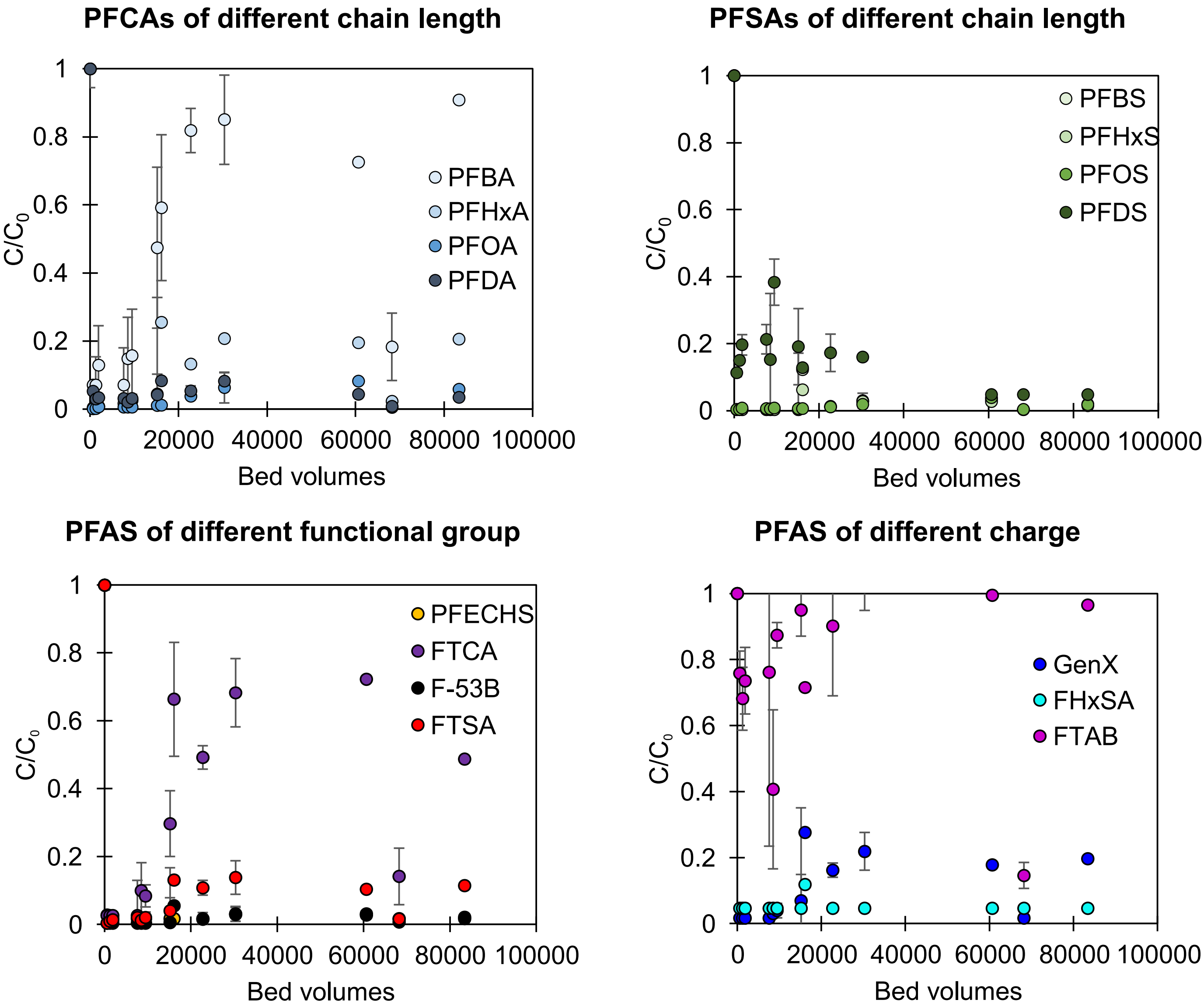

Figure 10. PFAS concentrations using TP109 MP IEX resin in RSSCTs from groundwater 1. PFAS were spiked at 0.4 nM.

7. Membrane separation

The literature review identified that high PFAS rejections have been reported using dense membrane processes such as nanofiltration (NF) and reverse osmosis (RO). This section explores the efficiency of these two membrane types in removing PFAS from UK water sources.

7.1 Methodology

A HP4750 stirred cell assembly (Sterlitech Corp., Kent, WA, USA) was used for bench-scale membrane filtration experiments (Figure 11) with an effective membrane area of 14.6 cm^2. The flat sheet membranes were pre-cut and stored at room temperature in deionised water for at least 24 h before testing and the membrane samples were pressurised with deionised water for 2 h. Cross flow filtration conditions were maintained by a magnetic stirrer supplied with the cell and the feed samples were continuously stirred throughout the experiments. The permeate was collected from a separate stream while feed and concentrate remained in the cell. The total volume of the membrane module was 300 mL.

Figure 11. Membrane module used in the PFAS removal experiments.

Following the literature review, three types of nanofiltration membrane and two types of reverse osmosis membrane were used in the experiments. All are commercially available products and were supplied by FilmTec. The specification of the NF90, NF270 and DK nanofiltration membranes and XLE and BW30 reverse osmosis membranes is given in Table 5. In order to evaluate the effect of membrane configuration on PFAS rejection, the membrane unit was operated in dead-end and cross-flow modes. The experiments were performed in the same cell. Cross-flow conditions were maintained by initiating mixing in the cell, while dead end conditions were maintained by removing the magnetic stirrer from the cell.

Table 5. Characteristics of the membranes used in this research.

	Membranes (Polyamide TFC)	MWCO (Da)	Permeability (L/m^2/h/bar)
Nanofiltration (NF)	NF270	400	12.7
	NF90	100-200	10.6
	DK	150	8.2
Reverse osmosis (RO)	XLE	100	7.8
	BW30	98	3.8

7.2 Results

Initial tests were performed to identify the flux variation through the membranes at different operating pressures (Appendix A). Once the optimal pressure conditions were identified, membrane separation tests were undertaken to compare rejection efficiencies of PFCAs and PFSAs with NF and RO membranes (Figure 12).

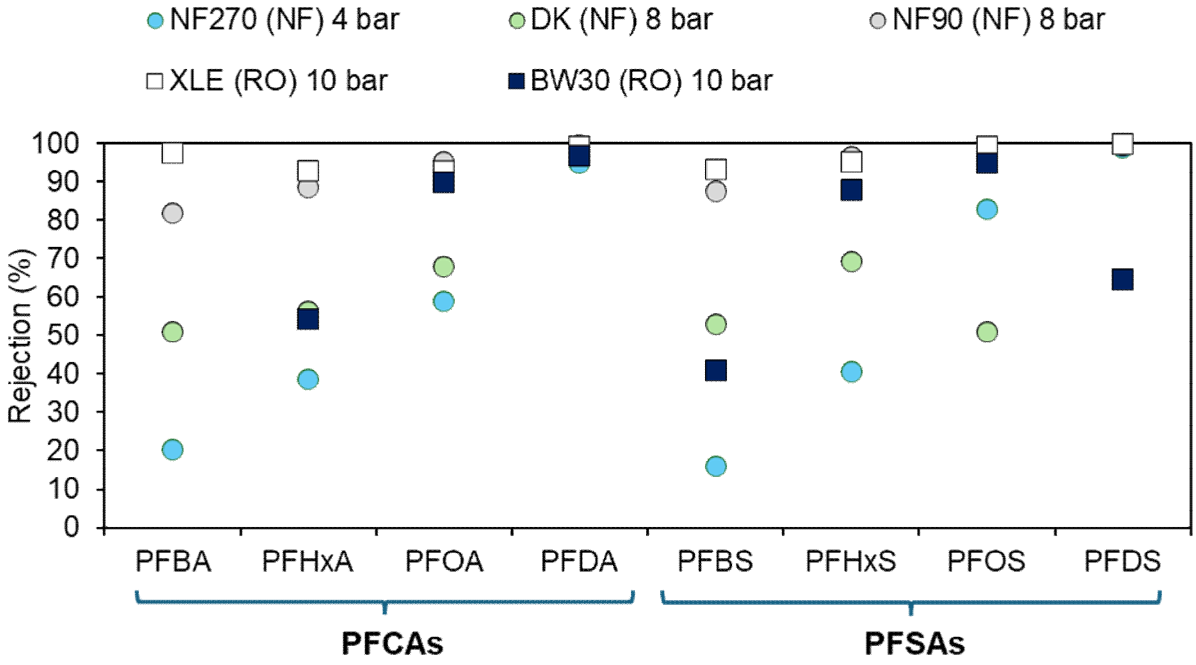

Figure 12. Rejection efficiencies of PFCAs and PFSAs by NF270, NF90, DK, XLE and BW30 membranes from groundwater 1. PFAS were spiked at 0.4 nM.

For all membrane types, the rejection increased with the molecular weight of the PFAS. PFSAs were better removed than PFCAs. The best performance was achieved with the XLE RO and the NF90 membranes, with rejection efficiencies reaching 99% for many of the

PFAS compounds. The XLE membrane was able to retain PFBA and PFBS, two of the shortest chain PFAS, by more than 90%. High removal rates were also seen for the NF90 membrane, with removal of 82 and 88% for PFBA and PFBS, respectively. PFDA and PFDS (10C) had the highest rejection rates, with over 95% achieved. This was explained by their high molecular weight limiting their passage through the membrane.

For PFAS of different functional group (Figure 13) but similar carbon number (8C), F-53B had the highest rejection, while PFOA had the lowest rejection, regardless of the membrane used. While PFOA was less well removed, the NF90 and XLE membranes were still able to remove the compound by >90%. The higher rejection of F-35B can be attributed to its higher molecular weight in comparison to the other PFAS compounds.

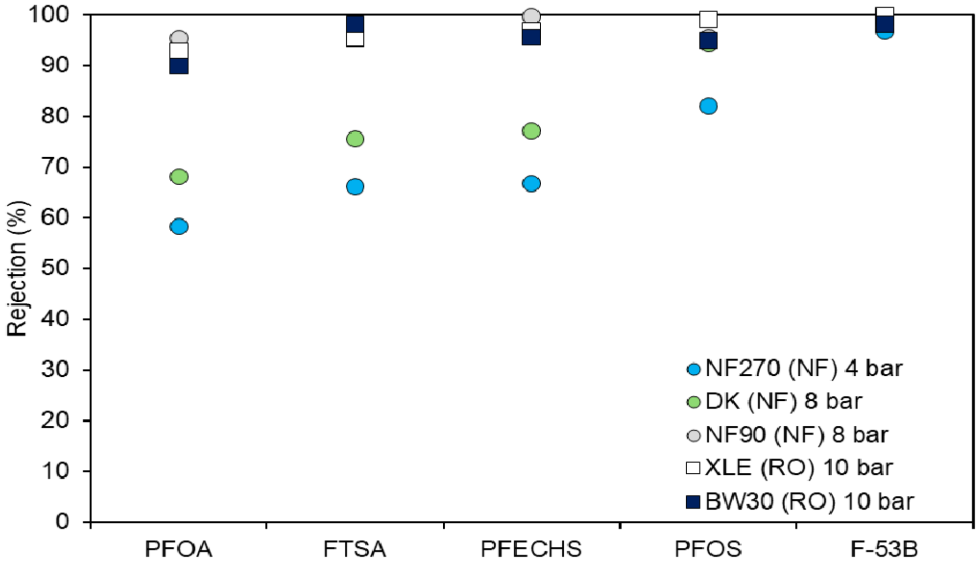

Figure 13. Rejection efficiencies of PFAS of different functional groups after filtration by NF270, NF90, DK, XLE and BW30 membranes from groundwater 1. PFAS were spiked at 0.4 nM.

When comparing the rejection of PFAS compounds of different charge (Figure 14), the highest rejection was again achieved with the NF90 and XLE membranes, with >90% removal observed for all the PFAS. Slightly lower removal of GenX was observed for the best performing membranes which may have been explained by its lower molecular weight and therefore increased passage through the membrane.

Following these results and considering the practicalities of applying different membranes into operational drinking water treatment applications, an NF membrane was selected to take forward for further study. This decision was based on the near similar performance of the membrane to the XLE RO membrane, and the lower operational pressure required to operate an NF system. As such, it was felt to be a more feasible option for broader full-scale implementation than an RO membrane option.

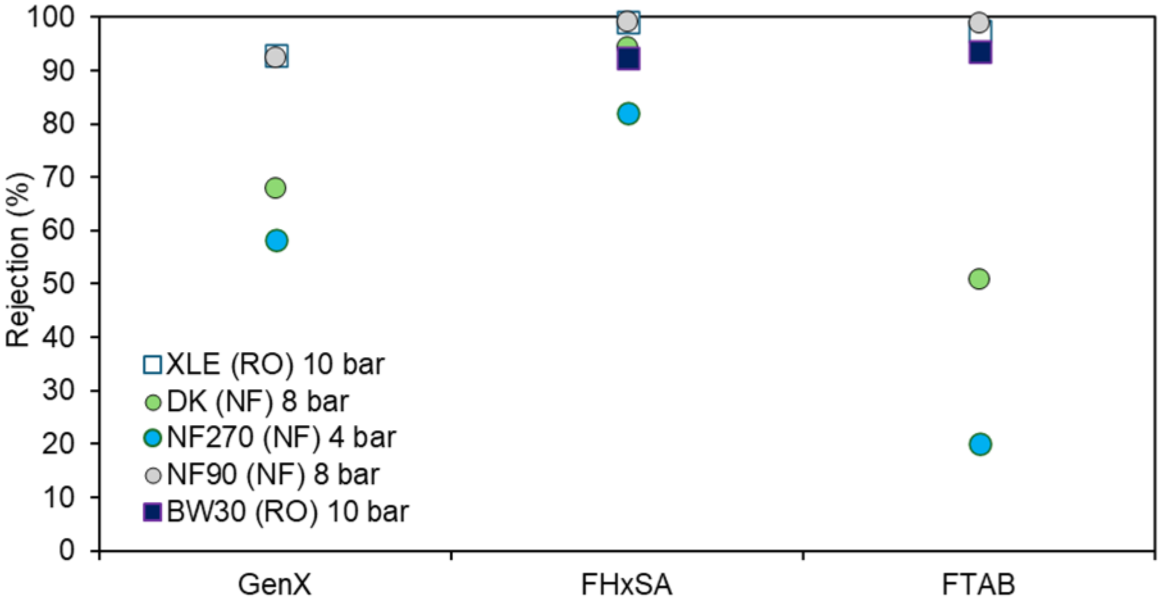

Figure 14. Rejection efficiencies of PFAS of different charge after filtration by NF270, NF90, DK, XLE and BW30 membranes from groundwater 1. PFAS were spiked at 0.4 nM.

Preliminary tests were performed to understand the influence of pH, humic acid and initial PFAS concentration on the membrane rejection (Appendix B). Subsequent tests investigating the impact of the inorganic ion valence on PFAS rejection (Figure 15) showed that shorter chain PFAS rejections were negatively impacted by the presence of ions with high valency. For example, decreasing from 81 to 52% for PFBA and 88 to 71% for PFBS with no ion addition to the addition of trivalent ions. This impact was reduced as the chain length increased, and PFDA and PFDS were not affected by the valence of the inorganic ions. This was posited to be as a result of a change in fouling layer characteristics that assisted the diffusion of smaller chain compounds through the membrane when highly charged ions were present. No significant differences were observed for rejection of PFAS of different functional group as the ion concentration changed. For PFAS of different charge, only the positive FTAB showed lower rejections in the presence of higher valence ions, decreasing from 99 to 77% in the presence of trivalent ions.

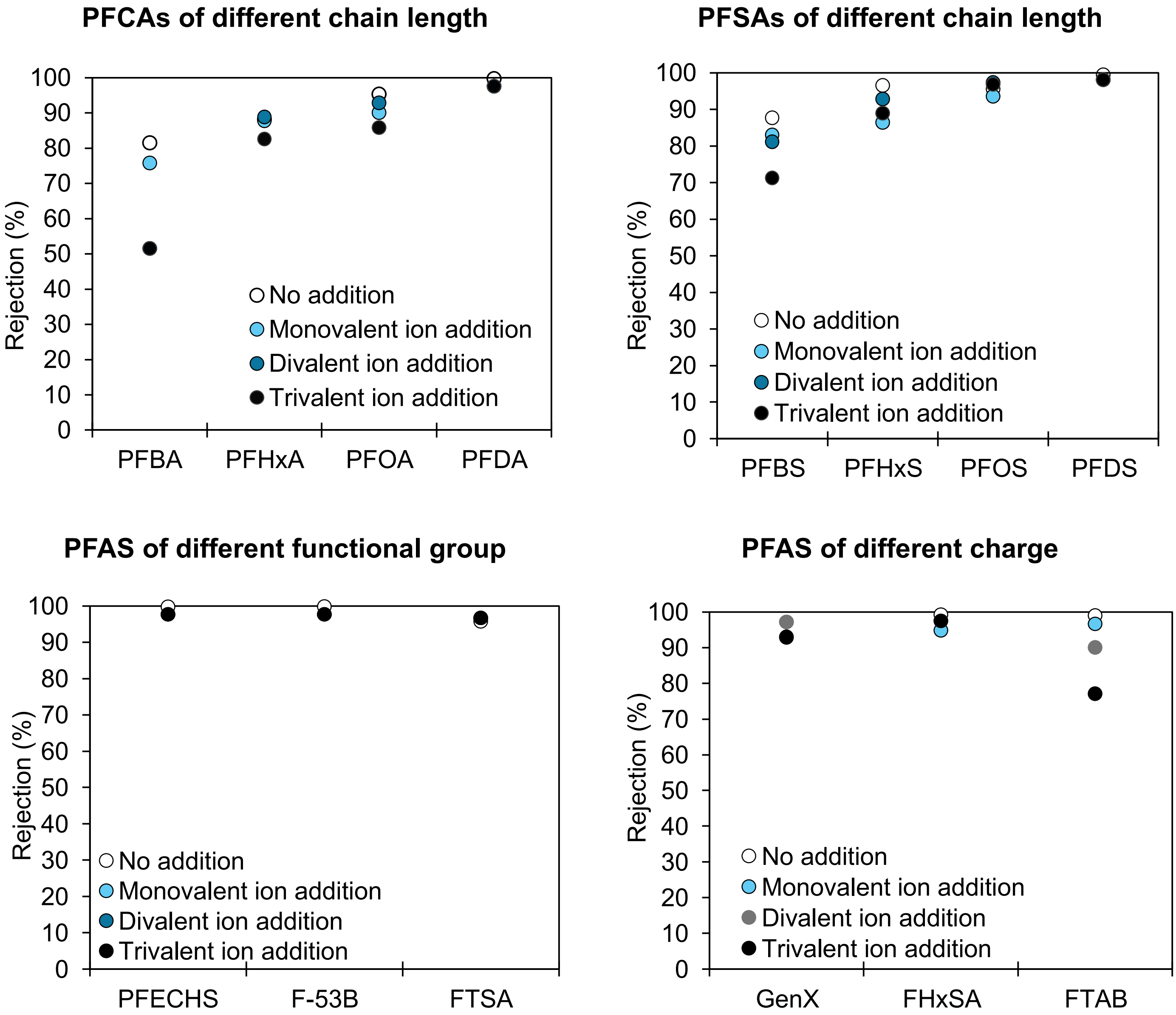

Figure 15. Influence of inorganic ion valence on PFAS rejection using NF90 in groundwater 1.

The performance of the NF90 nanofiltration membrane for PFAS removal was tested using 6 different water sources (Figure 16). The water characterisation data (Table 3) showed that lowland water 2 and the upland water had the highest organic matter concentration as indicated by the higher UV_{254} absorbance. Lowland water 2 also had the highest conductivity. In general, removal of PFCAs and PFSAs increased with increasing molecular weight as previously observed. The removal of PFSAs were slightly higher than for the PFCAs. However, there were differences in the level of removal achieved for the different water types. For example, the highest PFAS rejections of small PFAS were seen from groundwater 1 (81% for PFBA and 88% for PFBS), while for Source 5 less removal was observed (only 48% for PFBA and 64% for PFBS). Among the PFAS types of different functional group, F53-B was rejected by over 99% for all tested water types.

The rejection rate for GenX was between 58-63% for the waters from upland water, groundwater 3 and lowland water 2, while around 93% rejection was achieved from groundwaters 1 and 2. Similarly, FTAB rejection was between 83-95% from upland water, groundwater 3 and lowland water 2 and over 97% for groundwater 1 and lowland water 1. This was postulated to have been related to the higher organic matter content of the surface water sources, which can result in higher fouling, and thus, enhanced concentration polarisation, resulting in reduced overall removal.

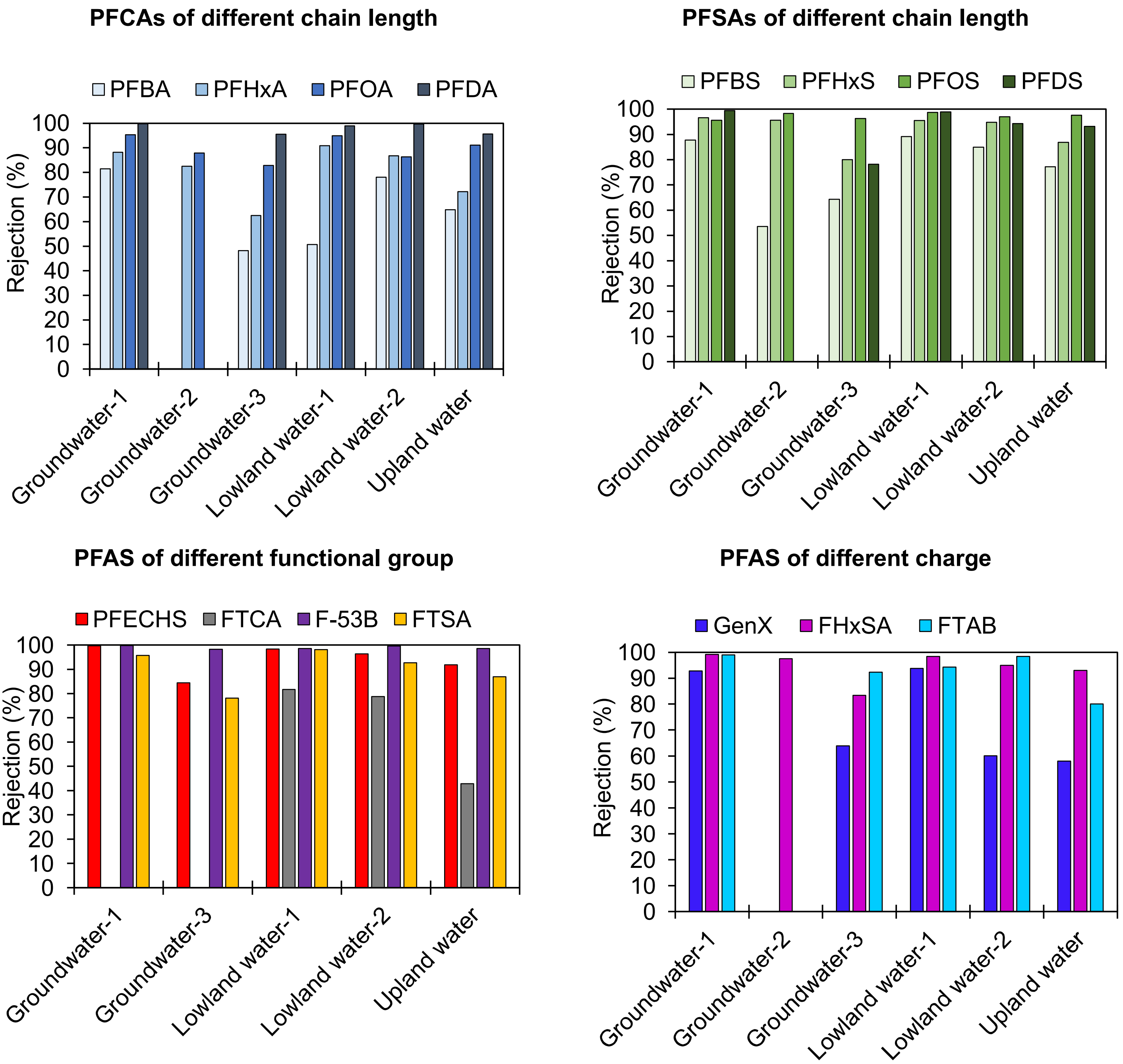

Figure 16. PFAS rejections by the NF90 membrane for different water sources. PFAS were spiked at 0.4 nM.

Overall, membrane separation showed high rejection rates for most PFAS compounds, where separation mechanisms include size exclusion, electrostatic interactions and hydrophobicity. The predominant mechanism was a function of the specific PFAS compound and the background water characteristics. While these results are encouraging, longer term operation of membranes is required to understand the influence of fouling on rejection efficiencies and flux over a longer operational period.

8. Advanced Oxidation/Reduction Processes (AOPs/ARPs)

AOPs and ARPs have been reported as waste-free destructive processes to remove PFAS. Although mechanisms of destruction vary, one of the proposed pathways is through the breakage of the C-F bond in the PFAS tail, which requires high photonic input. The other pathway is based on radical attack of the functional head group. The following section explores the removal of PFAS by photocatalysis, UV/H_2O_2 and UV/sulphite. UV/H_2O_2 is the most widely applied AOP for municipal applications. Photocatalysis can promote both oxidative and reductive reaction pathways through the formation of electron/hole pairs. UV/sulphite has recently gained traction as an ARP due to the use of sulphite, which produces innocuous sulphate during the process.

8.1 Methodology

ARPs and AOPs were performed in a Wedeco AG bench scale quasi-collimated beam apparatus (Herford, Germany) equipped with four 30 W UVC low pressure lamps emitting monochromatic light at 254 nm. The UV intensity was characterised using a radiometer and set at 20 W/m^2 (UV dose of 120 mJ/cm^2). A 250 mL Petri dish was used for the experiments, placed 22 cm from the light source and continuously stirred. UV/H_2O_2, UV/TiO_2, and UV/sulphite experiments were performed for 1 h. Hydrogen peroxide was dosed at a concentration of 20 and 40 mg/L, TiO_2 at a concentration of 100 and 200 mg/L, and sulphite at a concentration of 100 and 200 mg/L.

8.2 Results

Oxidation routes for PFAS degradation have only been demonstrated to be successful at high energy doses, and reductive routes may offer higher potential for PFAS removal (Bao et al., 2018; Cui et al., 2020). Results under all conditions and processes tested (Figure 17) saw PFAS removals below 20% for most of the compounds tested. FTAB, which was not well removed by IEX, showed removals between 28-72% for UV/sulphite and photocatalysis processes. FTCA also showed higher removal when using photocatalysis (between 29-73%). This could indicate a preference for these compounds to be removed through processes that offer a reductive pathway rather than an oxidative one.

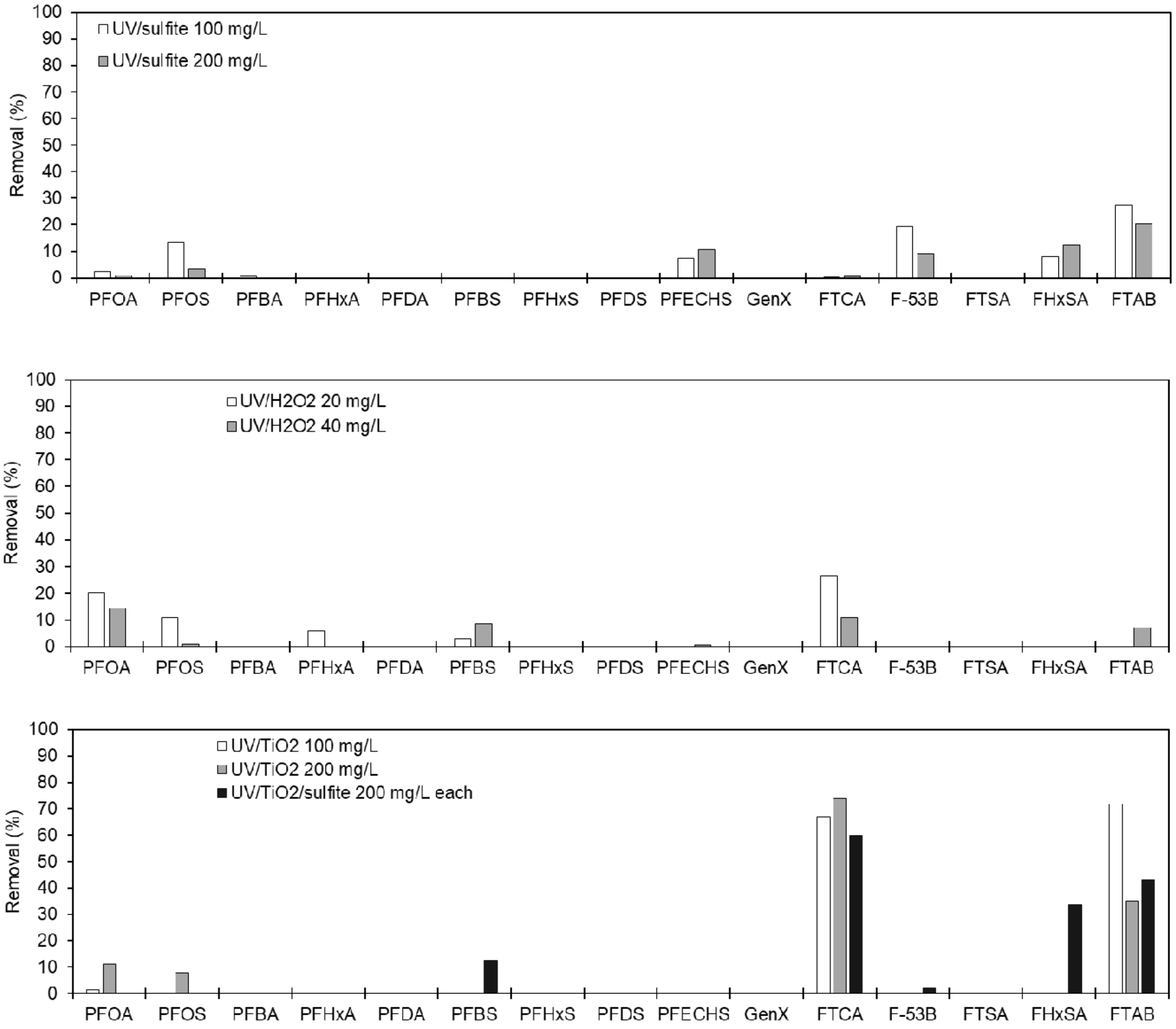

Figure 17. PFAS removal efficiencies with a) UV/sulphite at 100 and 200 mg/L; b) UV/H_2O_2 at 20 and 40 mg/L; and c) UV/TiO_2 at 100 and 200 mg/L and UV/TiO_2/sulphite at 200 mg/L. PFAS was spiked at 0.4 nM into groundwater 1.

Overall, however, AOPs and ARPs were the least effective way of removing a broad range of PFAS under the limited conditions tested here when compared to adsorption, IEX and membrane processes. No removal was achieved for shorter chain PFAS compounds or for the longer chain PFCAs or PFSAs. PFOA was removed by 20%, while PFOS was removed by <10%. Approximately 60-70% removal of FTCA was achieved with UV/TiO_2, which was much higher than that achieved by UV/sulphite and UV/H_2O_2 (0-26%). Between 40-70% removal of FTAB was achieved with UV/TiO_2, while this was between 20-30% for UV/sulphite and <7% for UV/H_2O_2. All processes and conditions tested were ineffective for removal of GenX, FTSA and PFECHS.

While the results presented do not show high removal efficiency for most PFAS, it is noteworthy that some conditions were effective for targeting specific PFAS (such as UV/TiO_2 for FTAB and F-53B). In addition, other types of ARPs and AOPs may be more suitable for PFAS removal at higher UV doses. For example, plasma-driven processes, supercritical water oxidation or electrochemical oxidation processes have been suggested as efficient processes to remove highly concentrated PFAS from water (Krause et al., 2021; Palma et al., 2022; Veciana et al., 2022).

9. Coagulation

Although it is not expected to be a process that offers significant potential for PFAS removal, understanding the fate of PFAS during coagulation is important as this process is frequently present at the front end of drinking water plants, particularly for those treating surface water sources. As such, the process is often the first to have contact with PFAS-containing water, hence understanding the extent of PFAS removal (even if this is unintended) is important to determine whether significant levels of PFAS enter water treatment sludge and whether this might then impact on its route for disposal. In this work, conventional iron and aluminium based coagulants were tested alongside novel chemicals that have previously been reported to provide increased opportunity for PFAS removal. For example, zirconium (Zr) salts are more highly charged (4+ valency), and precipitates of zinc (Zr) have been reported to be very hydrophobic.

9.1 Methodology

Coagulant chemicals used were: aluminium sulphate ($Al_2(SO_4)_3 \cdot 18H_2O$), ferric sulphate ($Fe_2(SO_4)_3 \cdot xH_2O$), zinc sulphate ($ZnSO_4 \cdot 7H_2O$), and zirconium chloride ($ZrOCl_2 \cdot 8H_2O$). sodium hydroxide (NaOH) and hydrochloric acid (HCl) were used for pH adjustment. The water source used for these experiments was from a brook local to Cranfield University (DOC: 3-6 mg/L DOC; UV_{254} absorbance: 0.032-0.045 cm^{-1}; turbidity: 5.6-6.3 NTU; alkalinity: 126-192 mg/L $CaCO_3$).

PFOA and PFOS were used as representative PFAS compounds to spike the water source. Both were added at concentrations ranging between 0.2-7 ng/L (0.001-0.04 nM) for PFOA and 0.2 ng/L (0.001 nM) for PFOS. Coagulation experiments were carried out on a PB-900 jar tester (Phipps and Bird, VA, USA). The mixing process included a 2 min rapid mix stage at 200 rpm, followed by 15 min flocculation at 30 rpm and a 20 min settlement period. Tests were carried out under pH conditions that lead to optimum charge neutralisation for the coagulant, and tests where no pH control was provided. Where the pH was adjusted, NaOH and HCl were used.

Further tests were carried out using the best performing coagulant (Al) under different pH conditions and increasing dose. PFOA and PFOS (2 nM of each) were spiked into the river water. The pH was adjusted to the required values (pH 4.5-6.5) and kept constant after coagulant addition by dosing NaOH and/or HCl during the rapid mixing stage.

9.2 Results

Under conditions of optimum charge neutralisation for each of the coagulants, PFOS was consistently removed when using the Al and Fe coagulants (Figure 18). In the case of Al, more than 20% PFOS removal was achieved for all doses tested, reaching a maximum of 27% for the highest coagulant dose. Lower removal was seen for Fe, with levels between 15-20% across the range of coagulant doses applied. The other coagulant chemicals did not see any significant removal of PFOS, other than 5-7% for the higher Zr doses. PFOA was poorly removed by all the coagulants under the charge neutralisation conditions.

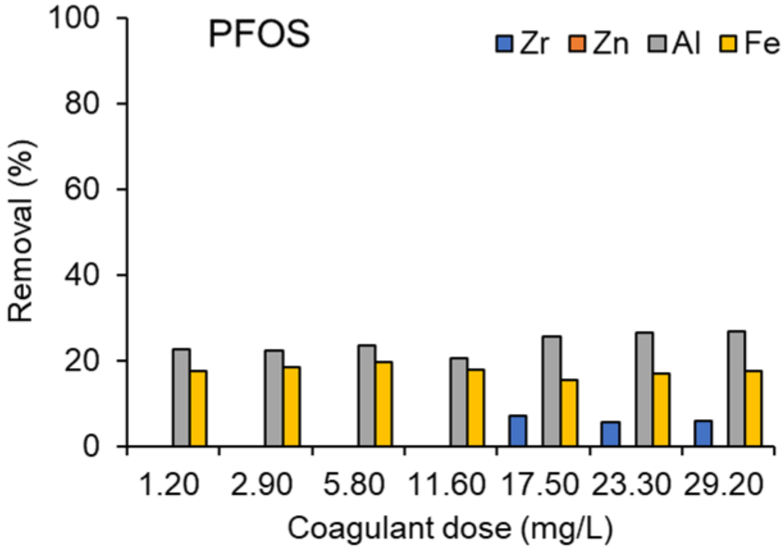

Figure 18. Removal of PFOA and PFOS by coagulants at increasing dose concentration with pH control (pH 4.5 for Fe and pH 5.5 for Zr, Zn, Al). PFOS and PFOA were spiked at 2 nmol·L^{-1} and 0.7 nmol·L^{-1}, respectively, into a brook water local to Cranfield.

When no pH control was applied into the coagulation experiment (in other words, the coagulant was dosed into the water without any pH adjustment chemicals), only the Al coagulant saw significant removal of PFAS at high coagulant doses, increasing from 10 to 58% at 17.5 to 29.2 mg/L as Al (Figure 19). This was coincidental with a switch from alkaline to acidic pH. Further coagulation tests where therefore carried out at three different pH (4.5, 5.5 and 6.5) using the Al coagulant to determine the role of pH on PFAS removal in a more controlled fashion (Figure 20). There was a clear pH effect, with more PFAS removal achieved under acidic conditions. At pH 4.5, removal of PFOS increased from 21 to 45% from the lowest to highest coagulant dose tested. Equivalent figures were 3 to 22% at pH 5.5 and less than 2% removal at pH 6.5. Lower overall removal was seen for PFOA, but the same effects were observed, with higher removal observed at the lower pH tested. Removal increased from 4 to 20% at pH 4.5, 0 to 11% at pH 5.5, and <2% at pH 6.5. These results show that pH played a strong role in the removal of PFAS by coagulation. It is posited that this is due to the hydrophobicity of the precipitates increasing at lower pH. The principal route for removal of PFAS during coagulation is through adsorption onto precipitate surfaces. For Al, under acidic conditions an amorphous and hydrophobic surface is formed during hydrolysis in water. This favours the possibility of hydrophobic and charge interactions to occur between the PFAS and the coagulant precipitate.

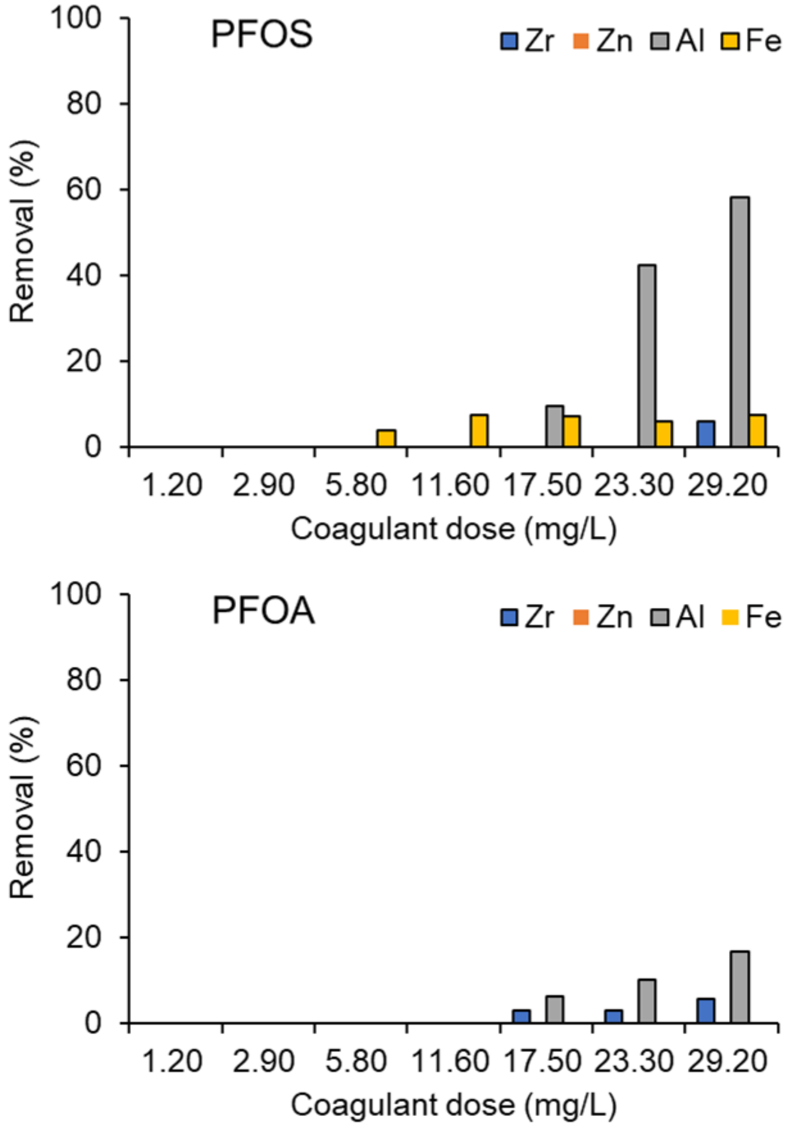

Figure 19. Removal of PFOA and PFOS by coagulants at increasing dose concentration with no pH control. PFOS and PFOA were spiked at 2 nmol·L^{-1} and 0.7 nmol·L^{-1}, respectively, into a brook water local to Cranfield.

While coagulation is not proposed to be a process for optimum removal of PFAS, these results show that some compounds can be removed during the process whether intended or otherwise. As a result, it is expected that where PFAS is present in the source water and where coagulation processes are in place at the water treatment works (WTWs), a significant proportion of PFAS will result in the drinking water sludge. In turn, this may influence the disposal options and management of the sludge waste.

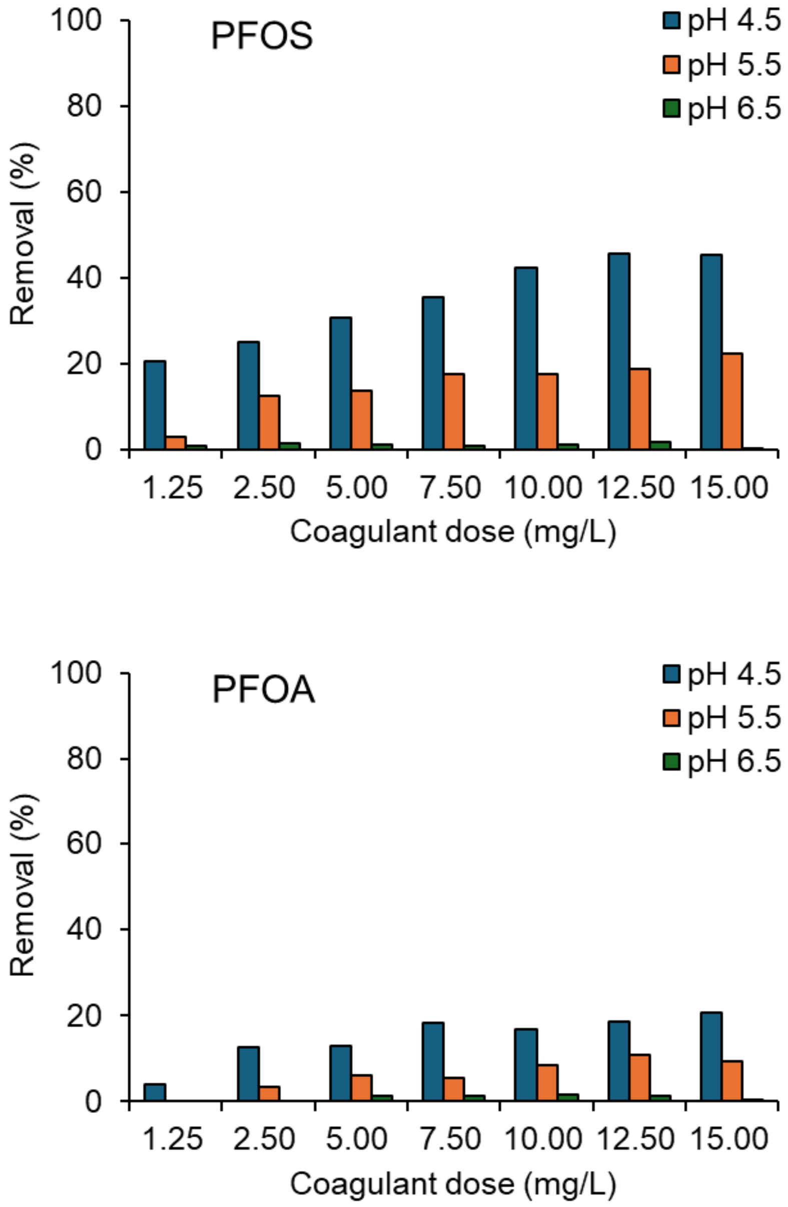

Figure 20. Influence of coagulation pH on PFOA and PFOS removal by Al coagulation with increasing dose. PFOS and PFOA were spiked at 2 nmol·L^{-1}, respectively, into a brook water local to Cranfield.

10. Summary

Comparison of the three most successful technologies tested for PFAS removal with respect to their main advantages and disadvantages is shown in Table 6 (adsorption, ion-exchange and membrane separation). In addition, for context, some indicative relative costs are presented that compare operational and capital costs for the different treatment processes assessed, applied to a small, medium and large sized WTWs. These in no way should be considered absolute as they have been taken from a US Environmental Protection Agency document (EPA, 2024), so they have an American context, and rely heavily on the water quality experienced by the process. Treatment costs will be dependent upon the extent of PFAS contamination, as well as other constituents present, local regulations, construction and materials costs, and disposal routes. There are also some unknowns around the potential efficacy for some processes. As such, these costings should only be used as an indicative and relative comparison.

The analysis indicates that:

- For GAC, costs are generally quite low (relative to the other processes) and become increasingly more beneficial as the size of the WTWs increases. Given that GAC infrastructure is often in place at many WTWs, capital costs may be minimal in many locations. However, this needs to be considered alongside the poor removal of small PFAS compounds, which may require more frequent media replacement/regeneration than is modelled here.
- For IEX, the process is the most competitive with respect to CAPEX and OPEX for small to medium sized WTWs.
- For membranes, this is the most expensive option for all sized WTWs and becomes increasingly less financially competitive as the size of WTWs increases. However, this should be considered alongside its performance, which typically provides the best removal of the widest range of PFAS compounds.
- More data is needed for the SMC media to provide an accurate cost estimate. For SMC, the required capital footprint and removal of PFAS compounds are estimated to be similar to those of IEX, with media cost sitting between GAC and IEX. As a novel media, further piloting should be performed to validate site-specific conditions.

Table 6. Summary table showing the key advantages and disadvantages for each of the different treatment processes, alongside estimated relative costs for capital and operational expenditure.

Process	Advantages	Disadvantages	Approximate costs*		
			WTW size	CAPEX	OPEX
Adsorption – Granular Activated Carbon	Moderate run times for removal of medium and high MW PFAS Very well known technology, often already in place at WTWs Media can be regenerated	Very low removal of small MW PFAS Although regenerable, some sites practice single use application of GAC Background contaminants can reduce PFAS removal - may require upfront treatment	3.8 MLD 38 MLD 380 MLD	£1.7million £7.0million £38.6million	£0.2million £0.9million £7.0million
Adsorption – Bentonite media	Long run times for effective removal of selected PFAS (PFOA and PFOS demonstrated here) Less affected by background contaminants than other sorbents	Unknown performance for range of PFAS in continuous mode of operation Disposal of media after single use Not approved for use in drinking water in the UK (although has NSF approval)	3.8 MLD 38 MLD 380 MLD	*No data available*	*No data available*
Ion-Exchange	Long run times before exhaustion for medium and high molecular weight PFAS Known technology (although not in the UK for PFAS removal and in single use operational mode)	Low removal of small MW PFAS Disposal of IEX resin after single use Background contaminants can reduce PFAS removal potential - may require upfront treatment Not all resins have approval for use in drinking water in the UK	3.8 MLD 38 MLD 380 MLD	£1.2million £5.4million £42.5million	£0.2million £1.5million £15million
Dense membrane filtration (nanofiltration or reverse osmosis)	High potential for removal of wide range of PFAS across all MW Known technology	Production of waste reject water (10-20% of flow) Membrane may require additional upfront treatment to protect membrane	3.8 MLD 38 MLD 380 MLD	£2.7million £9.3million £57.9million	£0.3million £2.3million £19.3million

*Approximated from a US EPA document (EPA, 2024), considering three sized water treatment works (3.8, 38 and 380 MLD). Modelled costs based on US context, for treatment of a PFAS contaminated groundwater. GAC considered in gravity operation (50,000 BV bed life), IEX in pressure vessels (120,000 BV bed life), membranes as reverse osmosis.

11. Conclusions and recommendations

The results presented in this report show the potential of GAC, SMC, ion exchange and membrane separation for effective PFAS removal for a range of different chemical species. However, each process had different efficiency towards a given PFAS compound. This is based on differences in the removal mechanisms and the physico-chemical properties of each PFAS compound.

- Conventional GAC was shown to be more effective in the removal of PFAS with chains of 6C or higher, with breakthrough occurring ca 10,000-13,000 BVs. However, it was not an effective barrier for PFBA and PFBS (4C carboxylic and sulphonic acids). Initial results with SMC show the potential for effective PFAS removal, but longer test runs are required (>9,000 BVs).
- For IEX, PFAS-specific Lewatit® TP109 MP provided the best results of the four resins tested, with higher BVs treated before breakthrough than was seen for GAC. Most PFSAs, PFECHS and F-53B were not seen to breakthrough even after the equivalent of 83,000 BVs. Most PFCAs, FHxSA, GenX, and FTBA showed breakthrough after 15,000 BVs. However, and similarly to GAC, IEX did not provide effective long-term removal of short chain (4C) PFAS (PFBA, PFBS).
- Membrane separation had the best removal of a broad range of PFAS. The nanofiltration NF90 membrane and the RO XLE membrane saw greater than 90% removal for most PFAS. Greater than 80% removal of short chain compounds were observed when using these membranes (PFBA, PFBS), as well as over 90% removal of GenX. A clear trend was observed where the longer the chain length for a given functional group, the higher was the removal efficiency, often reaching >99% removal for the largest PFAS compounds.
- Most AOPs and ARPs tested did not provide high removal efficiencies (max 30%) at the low UV doses tested. Only photocatalysis showed higher levels of removal for FTAB and FTCA (up to 70%).
- Under certain conditions, some coagulants could remove significant concentrations of PFAS from source water. Aluminium-based coagulants resulted in the highest removal (>15% for PFOA and >30% for PFOS), with

removal being favoured under acidic conditions and high dose. While coagulation is not recommended as a primary process for PFAS removal, the potential for the process to remove a range of compounds is important to acknowledge. Significant concentrations of PFAS may result in water treatment works sludge when PFAS is present in source waters, particularly when Al-coagulation is used as a treatment process.

- For many of the processes tested, the background water matrix did have an effect on removal. However, this was not always in a consistent way. For sorptive processes, higher concentrations of background DOC did not always result in earlier breakthrough of PFAS. This was linked to the nature and characteristics of the organic matter in each specific water source causing differences in the competition between these compounds and the PFAS for access to adsorption sites. For membrane processes, water types with higher DOC levels often resulted in reduced removal of some types of PFAS as a result of increased fouling and enhanced concentration polarisation, but this was not always the case.

The outcomes from the bench scale testing support the view that the pilot-scale phase of work should include GAC adsorption (F400), SMC, IEX (TP109 MP) and nanofiltration membrane separation (NF90). No clear trends in removal were observed across the different types of water matrices tested (groundwater, lowland and upland waters), but longer-term data during pilot testing was expected to provide a clearer effect of water constituents on removal profiles.

12. References

Bao, Y., Deng, S., Jiang, X., Qu, Y., He, Y., Liu, Y., Chai, Q., Mumtaz, Q., Huang, J., Cagnetta, G. and Yu, G. (2018). Degradation of PFOA Substitute: GenX (HFPO–DA Ammonium Salt): Oxidation with UV/Persulfate or Reduction with UV/Sulfite? *Environmental Science & Technology,* 52, 20, 11728–11734. DOI:10.1021/acs.est.8b02172.

Crittenden, J.C., Reddy, P.S., Arora, H., Trynoski, J., Hand, D.W., Perram, D.L., and Summers, R.S. (1991). Predicting GAC Performance With Rapid Small-Scale Column Tests. *Journal AWWA*, *83*(1), 77-97. DOI:10.1002/j.1551-8833.1991.tb07088.x.

Cui, J., Gao, P. and Deng, Y. (2020). Destruction of Per- and Polyfluoroalkyl Substances (PFAS) with Advanced Reduction Processes (ARPs): A Critical Review. *Environmental Science & Technology*, 54, 7, 3752–3766. DOI:10.1021/acs.est.9b05565.

Das, S. and Ronen, A. (2022). A Review on Removal and Destruction of Per-and Polyfluoroalkyl Substances (PFAS) by Novel Membranes. Membranes A Review on Removal and Destruction of Per-and Polyfluoroalkyl Substances (PFAS) by Novel Membranes. *Membranes,* 12, 662. DOI:10.3390/membranes15020064.

Dixit, F., Dutta, R., Barbeau, B., Berube, P. and Mohseni, M. (2021). PFAS removal by ion exchange resins: A review. *Chemosphere*, 272, 129777. DOI:10.1016/j.chemosphere.2021.129777.

EPA (2024) Technologies and Costs for Removing Per- and Polyfluoroalkyl Substances (PFAS) from Drinking Water, EPA Document No. EPA-815R24012 https://www.epa.gov/system/files/documents/2024-04/2024-pfas-tech-cost_final-508.pdf

Gao, Y., Deng, S., Du, Z., Liu, K., and Yu, G. (2017). Adsorptive removal of emerging polyfluoroalkyl substances F-53B and PFOS by anion-exchange resin: A comparative study. *Journal of Hazardous Materials*, *323*, 550-557. DOI:10.1016/j.jhazmat.2016.04.069.

Krause, M., Thoma, E., Sahle-Dmesessie, E., Crone, B.., Whitehill, A., Shields, E. and Gullet, B. (2021). Supercritical Water Oxidation as an Innovative Technology for PFAS Destruction. *Journal of Environmental Engineering*, 148, 2 1-8. DOI:10.1061/(ASCE)EE.1943-7870.0001957.

Kwon, Y.N., Shih, K., Tang, C. and Leckie, J.O. (2012). Adsorption of perfluorinated compounds on thin-film composite polyamide membranes. *Journal of Applied Polymer Science*, *124*(2), 1042-1049. DOI:10.1002/app.35182.

MPART. (2020). *Current Knowledge of Physiochemical Properties, Environmental Contamination and Toxicity of PFECHS Whitepaper*. Available at https://www.michigan.gov/-/media/Project/Websites/PFAS-Response/Workgroups/Human-Health/White-Paper-Physiochemical-Properties-Environmental-Contamination-Toxicity-PFECHS.pdf?rev=b86a48ec037549b29dbbace62c98fec8 [last accessed 20th February 2025].

Murray, C., Safulko, A., Vatankhah, H., Liu, C., Tajdini, B., Marshall, R.E. and Bellona, C. (2023). PFAS adsorbent selection: The role of adsorbent use rate, water quality, and cost. *Journal of Hazardous Materials,* 454, 131481. DOI:10.1016/j.jhazmat.2023.131481.

Palma, D., Richard, C. and Minella, M. (2022). State of the art and perspectives about non-thermal plasma applications for the removal of PFAS in water. *Chemical Engineering Journal Advances,* 10, 100253. DOI:10.1016/j.ceja.2022.100253.

Park, M., Wu, S., Lopez, I.J., Chang, I.Y., Karanfil, T. and Snyder, S. (2020). Adsorption of perfluoroalkyl substances (PFAS) in groundwater by granular activated carbons: Roles of hydrophobicity of PFAS and carbon characteristics. *Water Research*, 170, 115364. DOI:10.1016/j.watres.2019.115364.

Pérez-González, A., Ibáñez, R., Gómez, P., Urtiaga, A.M., Ortiz, I., and Irabien, J.A. (2015). Nanofiltration separation of polyvalent and monovalent anions in desalination brines. *Journal of Membrane Science*, 473, 16-27. DOI:10.1016/j.memsci.2014.08.045.

Phong Vo, H.N., Ngo, H.H., Guo, W., Hong Nguyen, T.M., Li, J., Liang, H., Deng, L., Chen, Z. and Hang Nguyen, T. A. (2020). Poly-and perfluoroalkyl substances in water and wastewater: A comprehensive review from sources to remediation. *Journal of Water Process Engineering,* 36, 101393. DOI:10.1016/j.jwpe.2020.101393.

Schaefer, C.E., Nguyen, D., Culina, V.M., Guelfo, J. and Kumar, N. (2020). Application of rapid small-scale column tests for treatment of perfluoroalkyl acids using anion-exchange resins and granular activated carbon in groundwater with elevated organic carbon. *Industrial & Engineering Chemistry Research*, 59(38), 16832-16837. DOI:10.1021/acs.iecr.0c02290.

Shen, J., and Schäfer, A.I. (2015). Factors affecting fluoride and natural organic matter (NOM) removal from natural waters in Tanzania by nanofiltration/reverse osmosis. *Science of the Total Environment*, 527–528, 520-529. DOI:10.1016/j.scitotenv.2015.04.037.

Shinagawa, T., Ohshima, H. and Kondo, T. (1992). Isoelectric point of an ion-penetrable membrane. *Biophysical Chemistry*, *43*(2), 149-156. DOI:10.1016/0301-4622(92)80029-5.

Soriano, Á., Gorri, D. and Urtiaga, A. (2019). Selection of High Flux Membrane for the Effective Removal of Short-Chain Perfluorocarboxylic Acids. *Industrial and Engineering Chemistry Research*, *58*(8), 3329-3338. DOI:10.1021/acs.iecr.8b05506.

Veciana, M., Braunig, J., Farhat, A., Pype. M., Freguia, S., Carvalho, G., Keller, J. and Ledezma, P. (2022). *Journal of Hazardous Materials* 434, 128886. DOI:10.1016/j.jhazmat.2022.12888.

Xiong, J., Hou, Y., Wang, J., Liu, Z., Qu, Y., Li, Z. and Wang, X. (2021). The rejection of perfluoroalkyl substances by nanofiltration and reverse osmosis: Influencing factors and combination processes. *Environmental Science: Water Research and Technology*, 7(11), 1928-1943. DOI:10.1039/d1ew00490e.

Zaggia, A., Conte, L., Falletti, L., Fant, M., and Chiorboli, A. (2016). Use of strong anion exchange resins for the removal of perfluoroalkylated substances from contaminated drinking water in batch and continuous pilot plants. *Water Research*, 91, 137-146. DOI:10.1016/j.watres.2015.12.039

Zeng, C., Tanaka, S., Suzuki, Y. and Fujii, S. (2017). Impact of feed water pH and membrane material on nanofiltration of perfluorohexanoic acid in aqueous solution. *Chemosphere*, 183, 599-604. DOI:10.1016/j.chemosphere.2017.05.132

Appendix A

Flux variation at different operating pressures

Membranes were operated under two different pressure values. The applied pressures were 4 and 8 bar for the NF270, NF90 and DK and 8 and 10 bar for the XLE and BW30 RO membranes (Figures A1 and A2). Low molecular weight cut off (MWCO) values given in Table 5 indicate that the membrane has a dense structure, and high values indicate that the membrane has larger pores that can allow more water to be filtered.

NF270 membrane had a higher MWCO, and a higher flux compared to the NF90 and DK membranes (Figure A1). The flux is a design parameter for scale-up of the process which also influences removal rates, energy consumption, membrane cleaning requirements. It is also an indicator of the amount of water that is filtered per unit time through per unit membrane area. Higher flux values were achieved at higher pressure values.

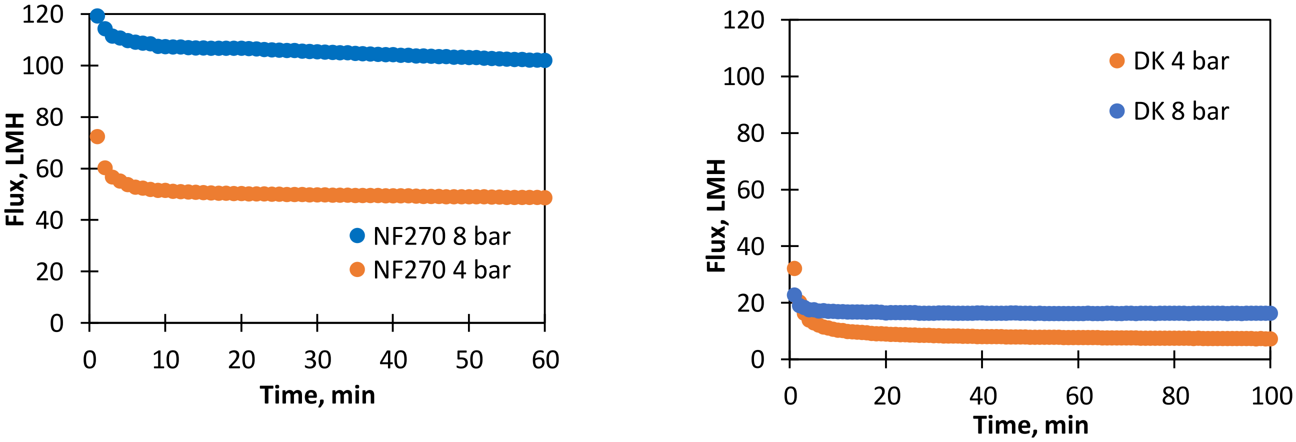

NF270 **DK**

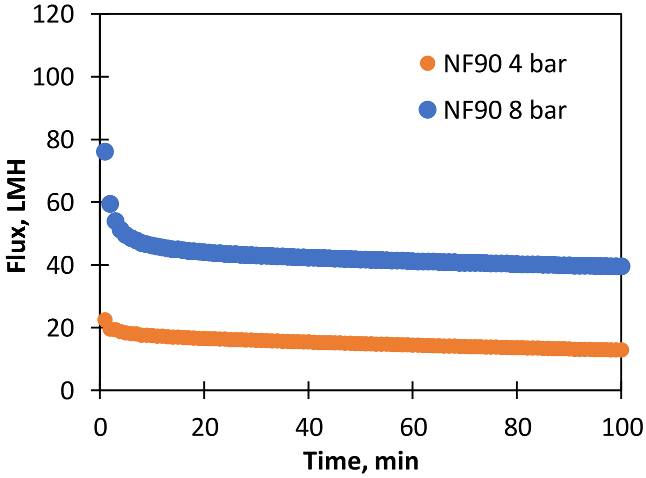

NF90

Figure A1. Flux variation of NF270, DK and NF90 nanofiltration membranes at 4 and 8 bars.

The flux of the nanofiltration membranes were valued around 50, 10 and 20 LMH under 4 bar pressure and when the applied pressure increased to 8 bar flux values were increased to 110, 20 and 40 LMH for NF270, DK and NF90 membranes respectively. The results were in line with previous studies and the permeability data of the manufacturer (Pérez-González et al., 2015; Shen & Schäfer, 2015; Soriano et al., 2019).

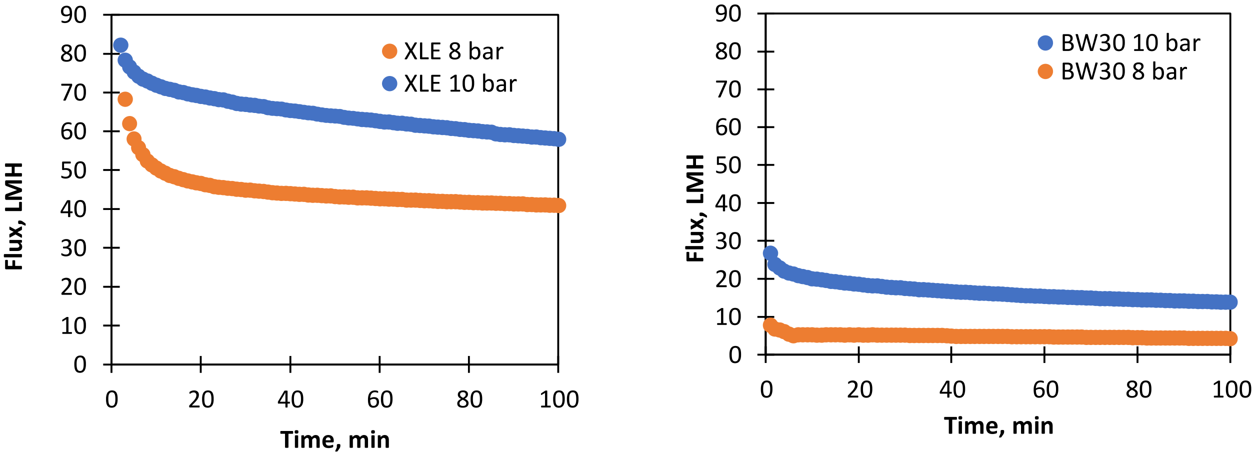

XLE **BW30**

Figure A2. Flux trend of XLE and BW30 reverse osmosis membranes at 8 and 10 bar of applied pressure

Similar data was achieved with RO membranes (Figure A2) as higher flux values were recorded at higher pressure values. This aligns with values reported in the literature (Soriano et al., 2019). With the XLE membrane even higher flux values were achieved. Under 8 bars of pressure the flux of the XLE membrane was ca 50 LMH and increased to 70 LMH at 10 bars, and for BW30 the flux increased from 5 to 20 LMH as the pressure increased from 8 to 10 bar.

Effect of pressure for the removal of PFOS/PFOA

The operating pressure for the membrane testing was based on the rejection of the PFOS and PFOA (Figure A3). The rejections for both PFOS and PFOA was highest with the NF90 membrane. Higher pressure resulted in higher rejection rates due to increased applied pressure leading to the spread of PFAS over the membrane surface, reducing the sorption effect. The exception was for the NF270 membrane which showed that PFOA rejections were lower than for PFOS, a result that was consistent with previous work (Kwon et al., 2012). Although PFOS and PFOA have the same number of carbon atoms, PFOA has a lower molecular weight and hydrophobicity than PFOS. Therefore, PFOS was more likely to be rejected compared to PFOA.

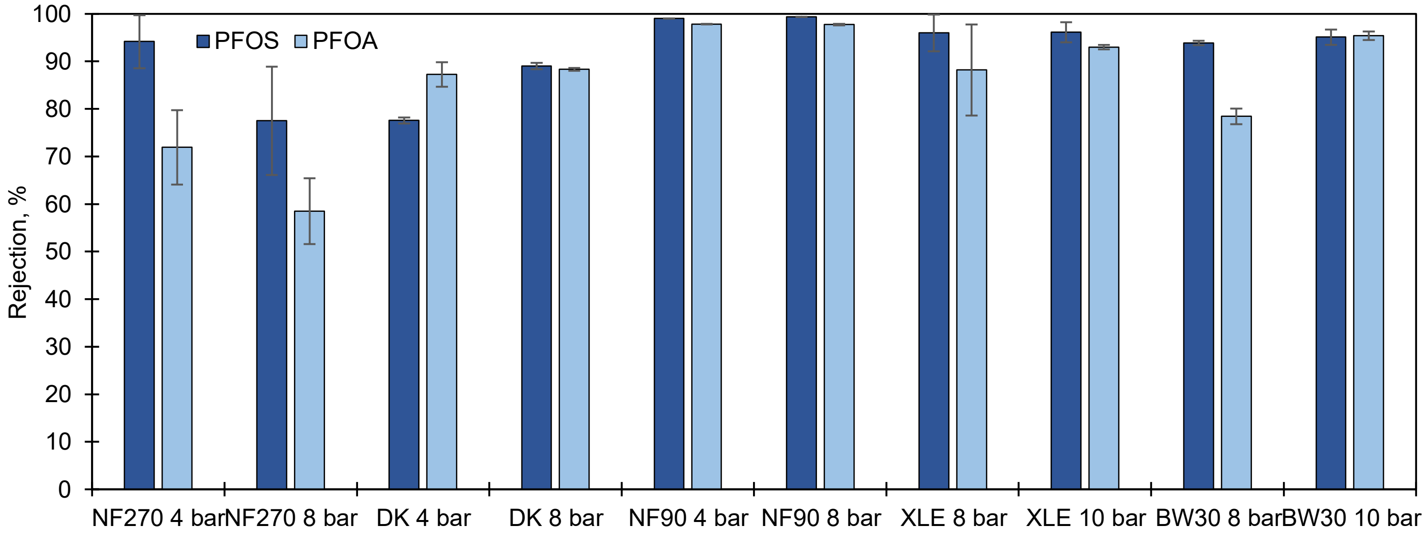

Figure A3. Rejection of PFOS and PFOA for NF270, NF90, DK, XLE and BW30 membranes.

Appendix B

Effect of pH

Changes in pH influence electrostatic separation mechanisms by affecting the membrane isoelectric point, surface charge and hydrophobicity. To investigate whether pH changes in the water matrix affects PFAS rejection, experiments were conducted with groundwater samples at 3 different pH values (pH 3, 7, 10) (Figure B1). The rejections were highest at pH 7 for both PFOS and PFOA which could be because of the isoelectric point of the NF90 membrane is close to neutral pH values. The isoelectric point of the membrane is defined as the pH at which the net charge of the membrane is zero (Shinagawa et al., 1992). At a pH value below the isoelectric point, the surface of the membrane is positively charged, resulting from the protonation of the amine groups ($NH_2 \rightarrow NH_3^+$). Above this point, it becomes increasingly negatively charged due to the deprotonation of carboxyl groups ($COOH \rightarrow COO^-$) and is stabilised at neutral pH (Zeng et al., 2017). As the surface becomes positively charged at pH 3, negatively charged PFAS molecules are attracted to the surface which also explains the lower rejections achieved at pH 3.

Carboxylic and sulphonic acids, including 4 carbon PFBA and PFBS) showed a different influence of pH on the rejection rates. PFBA was completely removed at low and high pH values, while it was only rejected by 81% at pH 7. PFBS was rejected at 50% at pH 3 and 40% at pH 10, with the highest rejection at pH 7 (90%). It was also seen that increasing chain length increased the rejections both for perfluoro carboxylic and sulphonic acids regardless of any change of the pH and the highest rejections were achieved for PFDA and PFDS (ca 98%). Over 90% rejection rates were achieved for PFAS with other functional groups (PFECHS, FTSA and F-53B) and the rejections were stable at different pH values. PFAS compounds representing the same chain length but different charge (GenX, FTBA and FhxSA) were well removed at pH 3 and pH 7, but rejection decreased at pH 10.

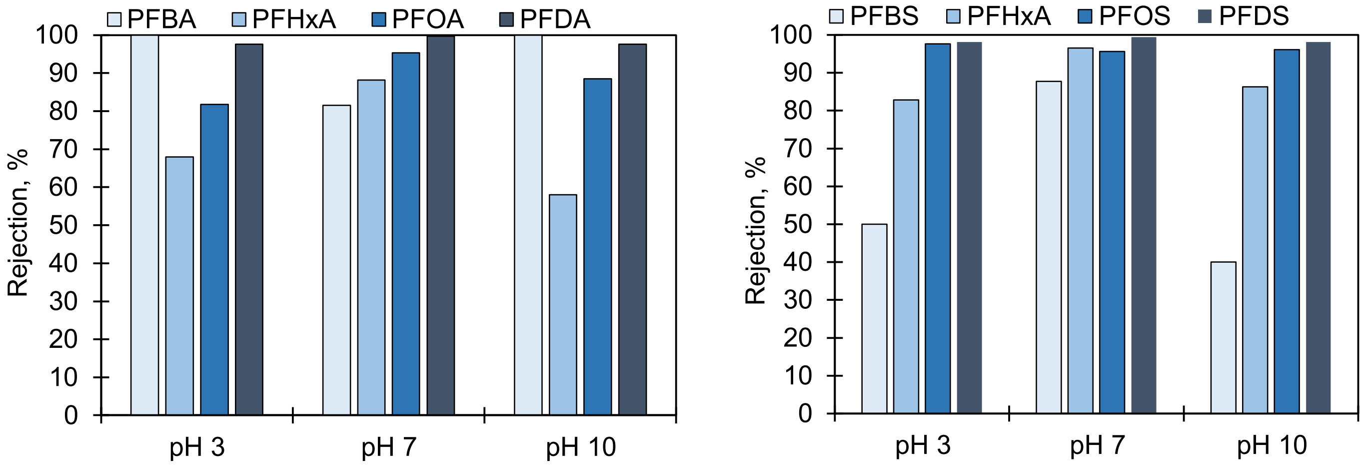

PFCAs of different chain length

PFSAs of different chain length

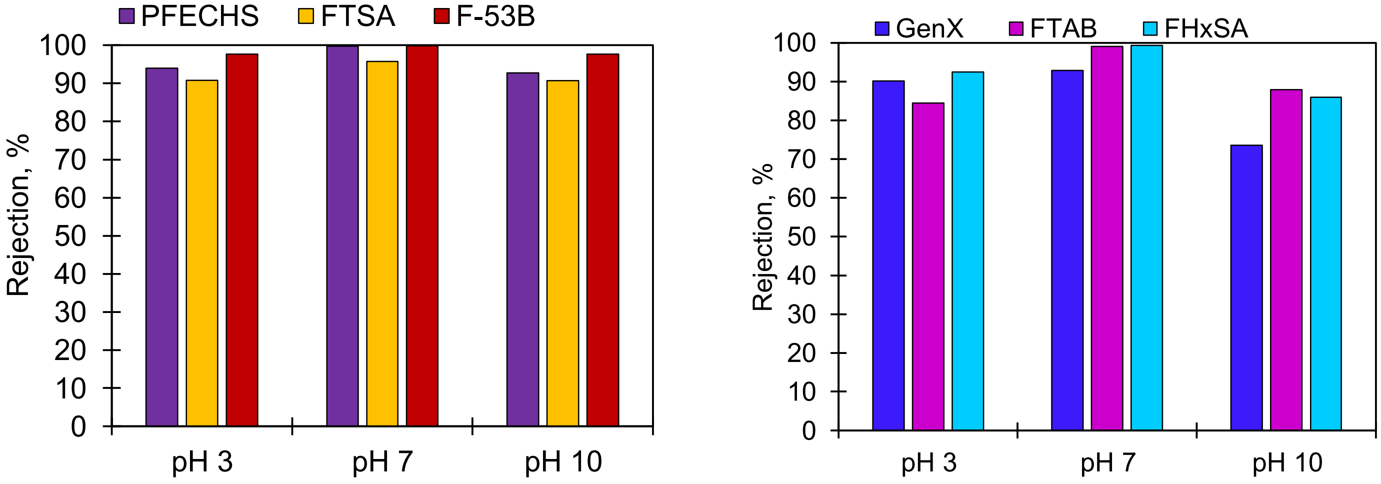

PFAS of different functional group

PFAS of different charge

Figure B1. PFAS rejections at pH 3, pH 7 and pH 10.

Effect of humic acid

Humic acid (HA) is a representative group of organic compounds, similar to that which is present in natural water (Dixit et al., 2021). The presence of organic matter in the water matrix can cause bridging between organic matter and PFAS molecules, resulting in an increase in the size of the PFAS-organic structure and the potential for more effective sieving mechanisms for removal by the membrane. There could also be adsorption of PFAS onto the added organic surfaces. In order to see the change on membrane performance 10 mg/L humic acid was added to the groundwater samples together with the PFAS compounds (Figure B2).

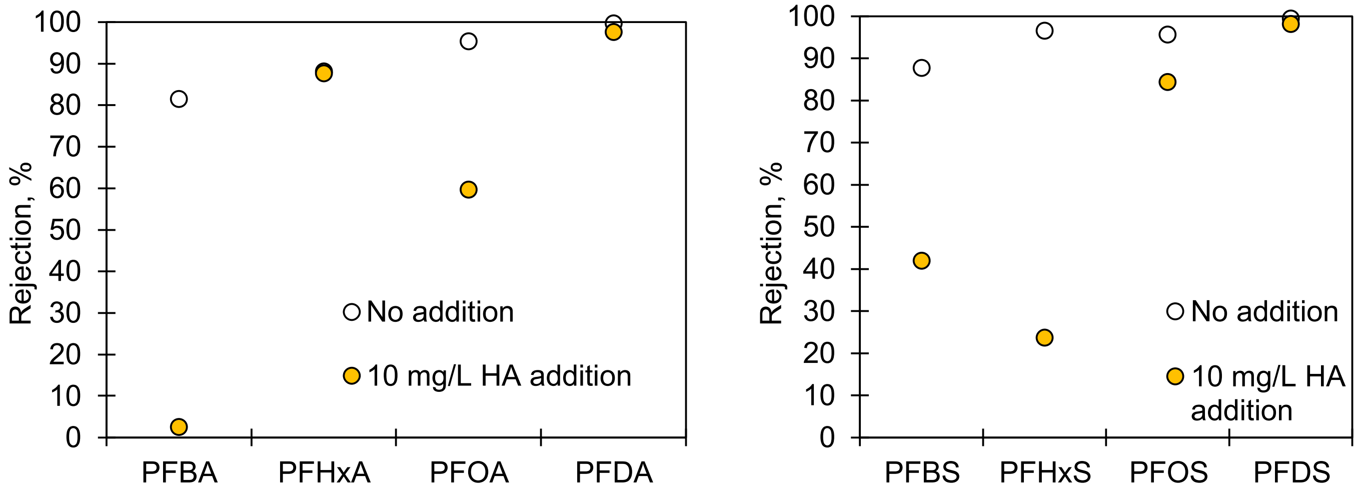

PFCAs with different chain length

PFSAs with different chain length

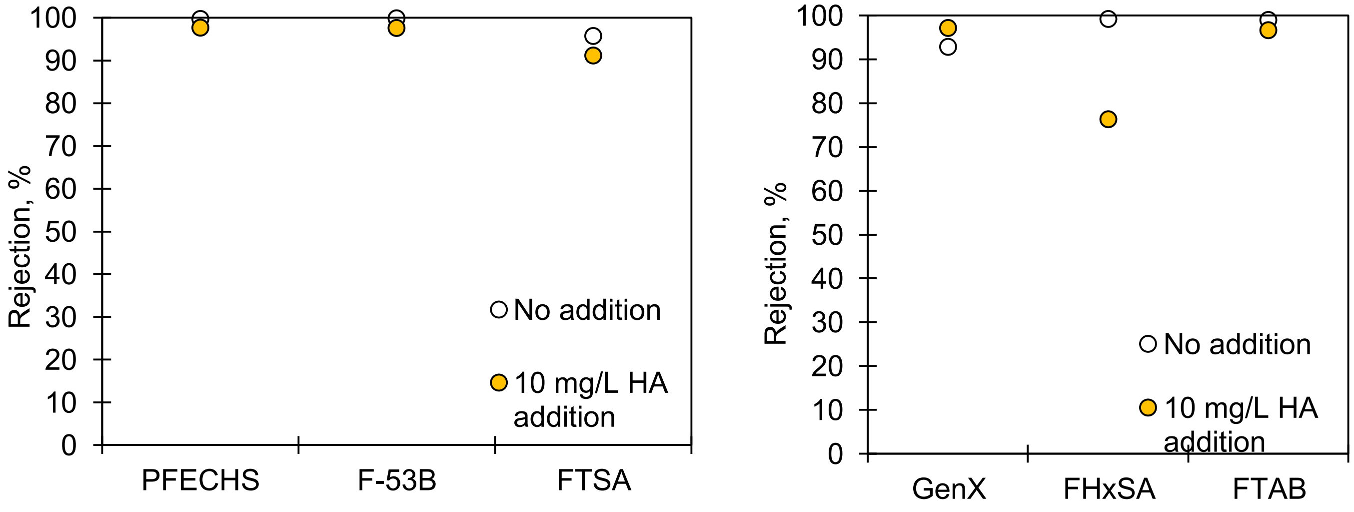

PFAS with different functional group

PFAS of different charge

Figure B2. PFAS rejections with 10 mg/L humic acid in groundwater.

The matrix plays an important role in controlling the effectiveness of PFAS removal. DOC is typically present at concentrations of at least one or two orders of magnitude higher than the PFAS. The separation mechanisms are more complicated by the presence of organic compounds and interactions with other constituents (Xiong et al., 2021; Phong Vo et al., 2020). Micelles or hemi-micelles might form on the membrane surface at relatively high PFAS concentrations. PFAS micelles are responsible for decreasing the favourable effects of fouling enhanced concentration polarization (Das & Ronen, 2022). PFOA and PFOS rejections decreased to 60% and 84% respectively. A size exclusion mechanism was only observed on the longest chain compounds: PFDA and PFDS were rejected at a rate of 98%.

For the shortest chained sulphonic and carboxylic acids, almost no removal was achieved for PFBA, while 42% removal was achieved for PFBS.

PFAS with other functional groups were less affected by the increased background organic content in the water matrix, with 97% rejections achieved for PFECHS and F-53B and 91% for FTSA. Positively charged FTAB and negatively charged GenX were efficiently removed at a rate of 97%. However, the rejection of neutral FHxSA was decreased from 99% to 76% by the addition of organic compounds.

Effect of initial PFAS concentration

Separation using the NF90 membrane was tested at higher initial PFAS concentrations (Figure B3). Figure B3 presents the rejection of PFOS and PFOA in comparison with the rejections achieved at 0.4 nM concentration. A similar set of experiments were performed with the model compounds (Figure 30). The rejection of PFOS increased from XX% to 99% as the PFAS concentration increased from 0.4 to 0.8 nM.

An increased PFAS concentration can lead to increased adsorption onto the fouling layer via hydrophobic interactions (Das & Ronen, 2022). It has been proposed that higher PFAS concentrations promote the attachment of both PFOS and PFOA to the membrane surface or entrapment in the membrane pores, leading to pores being narrowed or even blocked. In this case the rejection mechanism is dominated only by the membrane surface and PFAS-PFAS interactions. Hence, size exclusion effects can be stronger, improving the rejection of both PFOS and PFOA. In the presence of other PFAS compounds, the rejection of PFOA decreased from 95 to 62% while the rejection of PFOS remained approximately the same. Similar to the previous results, size exclusion mechanisms were more evident for the longest chained sulphonic and carboxylic acids PFDA and PFDS. Lower rejections were recorded for all other PFCAs and PFSAs except PFOS. PFECHS and FTSA were less likely to be removed at increased PFAS concentrations while the removal rate of F53-B remained at similar levels. When comparing the effect of charge on removal, the membrane performance decreased for GenX, FHxSA and FTAB, which indicated that the electrostatic rejection mechanisms were hindered. That could be related to the accumulation of PFAS compounds on the membrane surface resulting in diffusion of PFAS compounds to the permeate side due to the concentration gradient between the membrane and the solution.

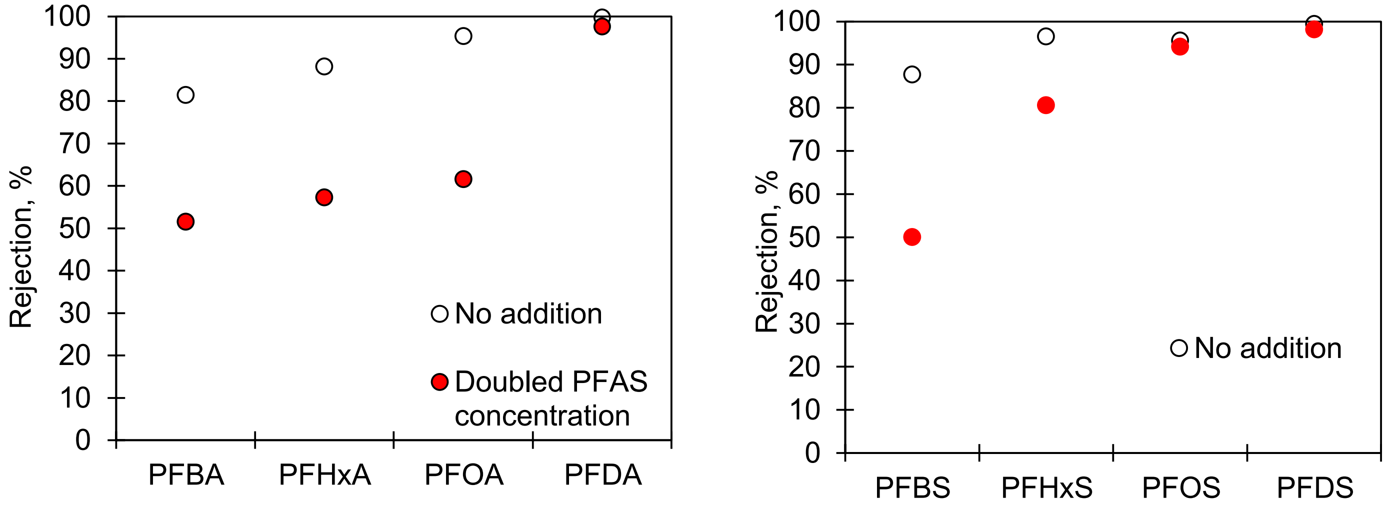

PFCAs with different chain length

PFSAs with different chain length

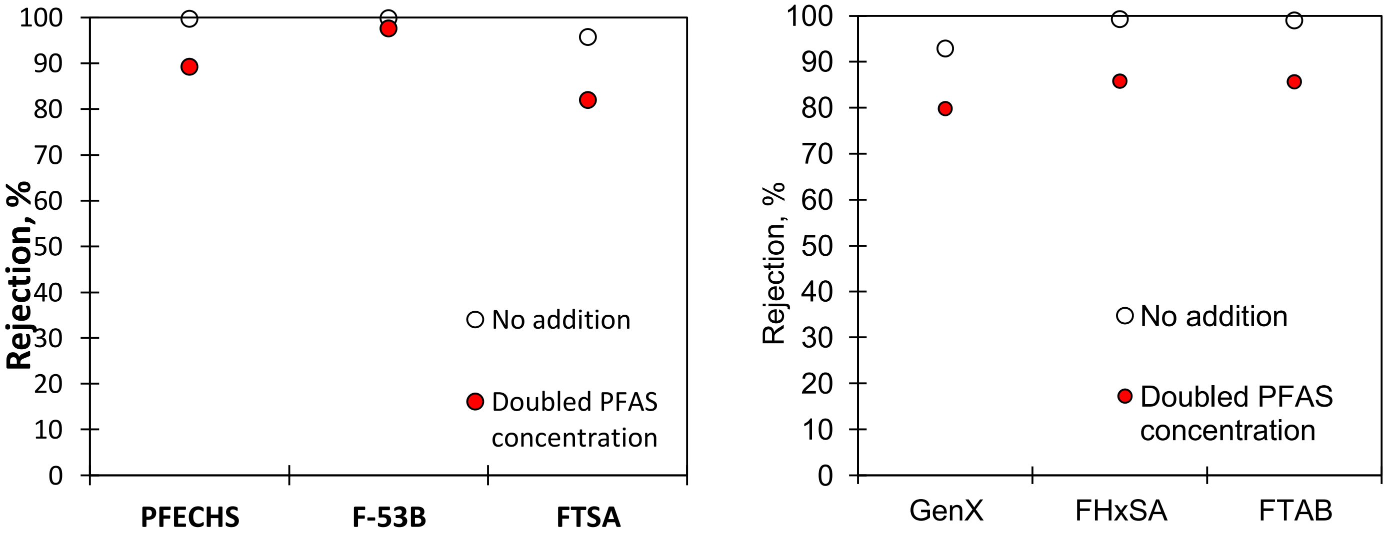

PFAS with different functional group

PFAS with different charge

Figure B3. PFAS rejection with 0.4 nM or 0.8 nM initial concentration in groundwater.